GENE REGULATION IN BIOFILMS

A Thesis
Submitted to the Graduate Faculty
of the
North Dakota State University
of Agriculture, and Applied Science

By

Priyankar Samanta

In Partial Fulfillment of the Requirements
for the Degree of
MASTER OF SCIENCE

Major Department:
Veterinary and Microbiological Sciences

August 2011

Fargo, North Dakota

North Dakota State University

Graduate School

Title

Gene Regulation in Biofilms

By

Priyankar Samanta

The Supervisory Committee certifies that this ***disquisition*** complies with North Dakota State University's regulations and meets the accepted standards for the degree of

Microbiology

MASTER OF SCIENCE

ABSTRACT

Samanta, Priyankar, M.S., Department of Veterinary and Microbiological Sciences, College of Agriculture, Food Systems, and Natural Resources, North Dakota State University, August 2011. Gene Regulation in Biofilms. Major Professor: Dr. Birgit Prüß.

Sessile bacterial communities which form on the solid surface or solid-liquid interface are known as biofilms. Both single species and multispecies biofilms are characterized by an extracellular matrix of polymeric substances which gives them several hundred times more antibiotic resistances than a planktonic bacterial culture. Though bacteria are the most common causative agent of various diseases, because of the high antibiotic resistance, biofilms cause complications of various diseases like cystic fibrosis, prosthetic valve endocarditis, chronic pulmonary diseases, catheter-associated urinary tract infections and several other diseases. From past studies, quorum sensing has been established as a novel target mechanism against biofilms; in this study, the two-component signal transduction systems (2CSTSs) have been focused. Once better understood, 2CSTSs can serve as a novel drug target and prevention mechanism for biofilm associated diseases.

According to prior high-throughput experiments and phenotype microarray experiments by our lab, several 2CSTSs like OmpR-EnvZ, RcsCDB along with the global regulator FlhD/FlhC were hypothesized to have an important effect on various developmental stages of biofilm formation. From that past study, we postulated that acetate metabolism may be an important aspect for biofilm formation. In this study, we tested and confirmed this hypothesis. We observed biofilms formed by several mutants in 2CSTS, as well as mutants in acetate metabolism, using Scanning Electron

Microscopy (SEM). We found quantitative and qualitative differences in the biofilm of the acetate mutants when compared to their isogenic parental *Escherichia coli* strain. An additional mutation in *rcsB* with acetate mutant strains forms less clumpy biofilms whereas an additional mutation in *dcuR* results in the formation of less biofilms. So the structural and the quantitative differences of acetate mutant biofilms depend on additional mutations in *rcsB* and *dcuR*.

Though a number of studies have been done on the temporal gene expression within biofilms, spatial gene expression of the mature biofilm is a big gap of knowledge. The future aim of this study is to study the temporal as well as the spatial gene expression of different 2CSTSs in the biofilm. In my MS thesis, I have constructed selected promoter fused GFP/RFP plasmids and some other fusion plasmids were purchased from the promoter collections from Open Biosystems, lastly *E. coli* AJW678 bacterial strains were transformed with these GFP/RFP fused plasmids. A 96 well microtiter plate assay was performed to study the temporal expression from the promoters by quantifying the fluorescence intensity in the planktonic culture. According to this experiment, the highest expression of *flhD* was after 20 hours whereas, the expression of ompR increases up to 7 days, which indicates that the *flhD* expresses earlier than *ompR*. The decreasing phase of flhD expression was paralleled by the sharpest increase in *ompR* expression as phosphorylated OmpR is an inhibitor of *flhD* expression.

ACKNOWLEDGEMENTS

Taking this opportunity, I would like to thank my major adviser Dr. Birgit Prüβ, for not only giving me an opportunity to work in her lab but also, for being helpful and a constant source of guidance. I would also like to thank Dr. John McEvoy, Dr. Penelope Gibbs, and Dr. Michael Christoffers for serving on my committee. I am also thankful to Dr. Shelly Horne for her endless technical help during this research study. I would like to thank Jayma Moore for processing the electron microscopy samples. I am also thankful to Pawel Borowicz, for helping me to setup the fluorescence microscopy experiment. I would also like to thank all faculty members and staff for being there to help whenever I needed them and all the graduate students in Van Es for their positivity. Finally, I would like to thank my parents; without their constant support, I could never have achieved this success.

This project was funded by NIH grant (1R15AI089403) and an earmark grant on Agro-security through USDA/APHIS.

TABLE OF CONTENTS

LIST OF TABLES

LIST OF FIGURES

INTRODUCTION

A biofilm can be defined as single species or multispecies bacterial communities that grow on solid surfaces or solid-liquid interfaces. Different developmental phases, characterized by different phenotypes, contribute to biofilm formation. An extracellular matrix of polymeric substances, an important phenotypic characteristic of the maturation phase, makes biofilm thousand times more antibiotic resistant than planktonic bacteria (Potera 1998).

Since high antibiotic resistance has such a huge impact on human disease, biofilm research has increased rapidly over the past 15 years, including studies on the developmental stages of biofilms, communication within biofilms, and gene transfer within biofilm bacterial species. Other studies dealt with the mechanism of various diseases related to biofilms. From the past studies, quorum sensing, which is characterized as cell to cell communication of bacteria, has already been established as a novel target mechanism against biofilms. According to a past high-throughput experiment by our lab (Prüβ 2010), several two-component signal transduction systems (2CSTS) may also exert significant effects on biofilm formation. This includes the osmoregulator OmpR-EnvZ and the colanic acid activator RcsCDB, both of which affect the flagella activator and global regulator FlhD/FlhC. As an additional hypothesis from this experiment it was postulated that acetate metabolism was an important sensory mechanism, receiving signals from the environment and transmitting them to the cell which influence biofilm formation. In a first Specific Aim for this thesis, we will use electron microscopy and several mutants in 2CSTS, as well

as mutants in acetate metabolism, to test the hypothesis from the high-throughput experiment.

All of the previous studies averaged gene expression over the total biofilm. They did not consider biofilm as an individual model where biofilms consist of micro-niches that differ with respect to the environmental conditions that the bacteria are exposed to. In Specific Aim II of this thesis, we will focus on the temporal and spatial expression of selected 2CSTSs along with the global regulator FlhD/FlhC. Taking advantage of novel fluorescence microscopy techniques and fluorescence probes, the spatial as well as the temporal expression from those promoters will be studied. The goal of my master's thesis is to construct the fusion plasmids and get the initial fluorescence microscopy working. As a long term goal of this study, we are targeting 2CSTSs as they are only present in the bacterial system and not in the human body. We will propose 2CSTSs for the development of novel prevention and treatment techniques for biofilm-associated infectious diseases by identifying the particular 2CSTSs that are expressed during the early phases of biofilm formation (prevention), as well as the particular regulators that are expressed at the surface of the fully developed three-dimensional structure (treatment).

LITERATURE REVIEW

Biofilm is a complex aggregation of microorganisms that forms on a solid substrate or at a liquid-air interface. In nature, microbial biofilm is the result of irreversible attachment of the bacterial community to a submerged surface. After attaching to the surface, the bacterial community provides a sticky extracellular matrix of polymeric substances (EPS) which further enhances the adhesion to the surface and/or one another. Biofilms behave differently than planktonic organisms in various respects. As one example, biofilms are almost 1500 times more antibiotic resistant than planktonic cells (Wu 2003). Because of the high antibiotic resistance, biofilms are considered a public health issue.

1. Biofilm-Associated Problems and Applications

1.1. Biofilm-associated problems

Biofilms are highly abundant in nature; almost 90 percent of bacteria establish themselves in any environment by producing biofilms (Ferrières 2003). In any environment, both single species and multispecies biofilms can form, though multispecies biofilms are more abundant in nature. Biofilms can also form inside the human body and can contribute to different types of infectious diseases. According to the Center for Disease Control and Prevention (CDC), more than 65% of nosocomial infections are caused by biofilms. Biofilms can grow on dental surfaces, mucus layers of the respiratory track system, the urinary tract, as well as central venous catheter surfaces of the human body. Biofilm can also grow on the mechanical heart valve after heart surgery.

Table 1 lists some common diseases associated with biofilm. Some of these will be discussed in the following paragraphs.

Disease	Contribution to Biofilm	Contributing microorganism
Dental Plaque	Good solid-liquid-air substrate is favorable for biofilm formation	Any aerobic bacteria
Cystic Fibrosis	Affects lung and digestive tract by making a thick layer of mucus. Mucus layer is perfect for biofilm growth.	*Pseudomonas aeruginosa*
Prosthetic Valve Endocarditis	Biofilms can grow on the mechanical heart valves, as well as the surrounding tissues of mechanical heart.	*Staphylococcus epidermidis, Staphylococcus aureus,*
Central Venous Catheter Biofilm	Formation of biofilm on central venous catheter surface is universal but the amount of biofilm and duration time can affect our normal body flora and can cause bloodstream infection.	*S. epidermidis, S. aureus, P. aeruginosa,*
Chronic Pulmonary Disease	Biofilm stimulates neutrophils to release elastase. This inhibits the mucus-ciliary function in the airways.	*Haemophilus influenza, Streptococcus pneumoniae*

Table 1 ***Selected biofilm associated diseases.***

1. **Dental plaque.** The solid-liquid interface of the dental surface is a very favorable condition for a biofilm to grow. Initially, the biofilm layer on the dental surface is very soft. After 48 hours, it gets harder and after few days it becomes rock-hard dental plaque. In one study, at least 40 different bacterial strains were identified with a checkerboard DNA–DNA hybridization assay that contributed to the biofilm (Li 2004).

2. **Cystic fibrosis.** Biofilms also contribute to chronic diseases, such as cystic fibrosis (CF). CF is an inherited disease that affects the mucus level in lungs and the digestive tract. The CF transmembrane conductance regulator (CFCR) gene encodes a particular protein which controls the chloride ion channel in the human body. Though in the human body two copies of this CFCR gene are present, only one copy is sufficient to control that protein. But in the CF patient, both copies of the CFCR gene are mutated. As a result, the chloride ion channel does not work properly and the body salts stay inside the cell and cause hyper osmosis. As a consequence, water from the mucus layer of the digestive and respiratory tracks diffuses into the cell, which makes the mucus layer thicker and makes breathing more difficult. Furthermore, the thick mucus layer is a perfect place for the formation of biofilm, especially by microaerophilic and opportunistic bacteria, such as *P. aeruginosa* (Singh 2000). The EPS or the slime layers of the biofilm that the bacteria produce can cause additional respiratory problems for the CF patients (Marquisa 2008).
3. **Prosthetic valve endocarditis.** This disease is associated with mechanical heart surgery. Prosthetic valve endocarditis can occur after a mechanical heart transplant (Wang 2007). Biofilms can grow on the mechanical heart valves, as well as the surrounding tissues of the heart. The initial microorganism contamination can come from the invasive procedure or the indwelling device. *S. epidermidis, S. aureus,* and several species of *Enterococcus* or *Streptococcus,* as well as certain gram-negative *Bacilli* can cause prosthetic valve endocarditis (Donlan 2001).

In addition to the medical problems, biofilms can also cause problems in many other settings. As one example, biofilm can be involved in bio-corrosion and biofouling, when the biofilm forms on a metal surface. This is due to an electrical potential that forms between two areas within the biofilm that vary in their oxygen concentration. The anaerobic metallic region surrounded by the thick biofilm will then act as an anode and the metallic region under the aerobic environment acts as a cathode. In the case of sulphate-reducing bacteria, the biofilm reduces sulfate to hydrogen sulphide, which corrodes metal by producing metal sulphide as the corrosion product (Borenstein 1994). One example where bio-corrosion constitutes a big problem would be seashore gas and oil industries, which use metallic pipes. Biofouling has a significant effect in marine industry. This is caused by the attachment of marine organism to ship hulls. Once the bacterial biofilm is established, it will facilitate the attachment of other marine organisms, such as barnacles. As a result, the vessel speed will either be reduced by up to 20 percent or fuel consumption will be increased by up to 40 percent (Office of Naval 2009), paralleled by an increase in greenhouse gas emission.

Bioinvasions is another example where biofilm can be a cause of environmental pollution. Bioinvasions can occur by the biofilm from ships' ballast-water tanks (Drake 2007). In the internal surface of ballast tank, formation of both single species and multi species biofilm is very common but when these biofilms are removed into the sea water they can cause pollution by generating more biofilms. Most of the time, these biofilms contain potentially harmful bacteria, viruses, or algae (Drake 2007).

Due to this toxic bioinvasions caused by biofilm, the marine organisms are greatly affected.

1.2. Biofilm applications

Besides all these disadvantages, biofilms can be used for human benefits. Two such fields are energy production by microbial fuel cells and copper production by microbial leaching. Fig-1 shows a schematic diagram of a microbial fuel cell which contains an anode in the anaerobic anode chamber and a cathode in the aerobic cathode chamber. These two chambers are separated by a proton exchange membrane (PEM) which allows only protons to pass from the anode to the cathode chamber (Gil 2003). The anode is covered by biofilm, which uses the carbon component as an energy source to produce electrons. Electrons will then flow from the anode to the cathode through the attached resistance where they produce the renewal energy. The thicker the biofilm around the anode surface, the more electricity it will produce (Reguera 2006). The best investigated bacterial species that are used on the anode surface are *Clostridium, Shewanella* and *Geobacter*.

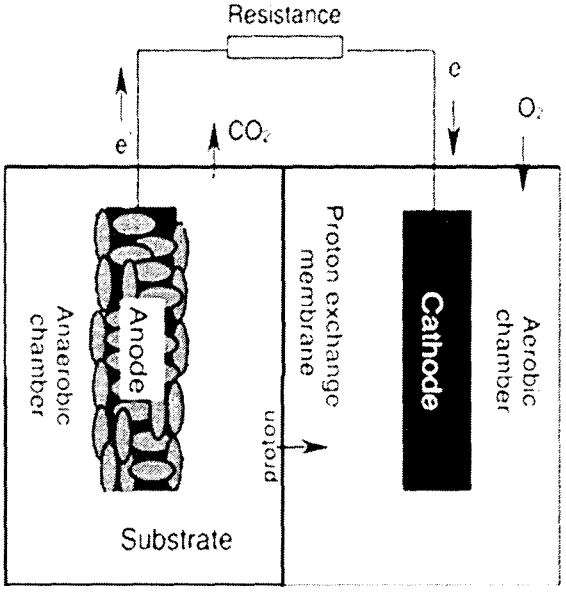

Fig - 1 ***Schematic diagram of a microbial fuel cell.***
MFCs made of one cathode chamber and one anaerobic anode chamber separated by PEM. Biofilms are grown on the anode surface.

Microbial leaching for copper production is another common field that is associated with biofilm. Almost eleven percent of the total copper production of the USA is coming from low grad copper ore by microbiological leaching of these ores. First of all, the surface of the copper ore is sprayed with water which makes the ore-water interface an appropriate environment for the biofilm formation. Then, a biofilm of bacteria, especially from the genus *Thiobacillus,* forms on the surface of the copper ore which contains several minerals. Oxidation of minerals like iron sulfide and other sulfides by the biofilms produces ferrous sulfate which is an oxidizing agent. This ferrous sulfate then oxidizes copper sulfides to release soluble $CuSO_4$. Copper can be extracted from this soluble $CuSO_4$ by solvent extraction (Sand 1995).

2. Gene Regulation in Biofilms

2.1 Phases of biofilm development

The formation of biofilm proceeds through several developmental stages, each of which is characterized by distinctly different phenotypes (Fig-2). The stages will be discussed in the following paragraphs:

At the very first stage of biofilm formation, planktonic bacteria loosely attach to a surface. This attachment is mediated by weak reversible van der Waals forces. During this time, bacteria can still leave the surface. After the weak attachment, bacteria can stick to the surface irreversibly by fimbriae and curli. The gene expression that is involved in this transition is called the swim or stick switch. Once bacteria irreversibly attach to the surface, they will form 3D, often mushroom-shaped, mature biofilms.

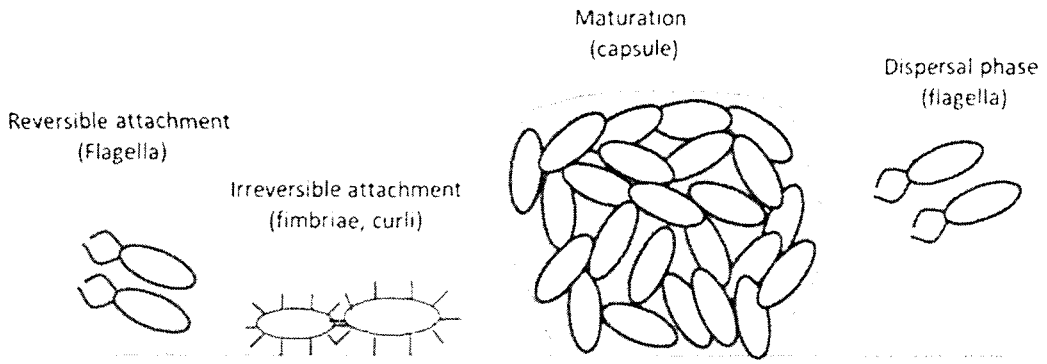

Fig - 2 ***Different stages of biofilm formation.***

Bacteria loosely attach to the surface with the help of flagella, which is called reversible attachment (or phase I). In the irreversible attachment phase (or phase II), bacteria strongly hold on to the surface by curli or fimbriae. In the maturation phase (or phase III), bacteria form the three-dimensional structures that constitute the biofilms. These bacteria are covered by the capsule. After the maturation phase, newly formed bacteria leave from the biofilm and become motile again with the help of their flagella. This is called dispersal (or phase IV) (figure modified from Monroe 2007).

In the maturation phase, biofilms are covered by an extracellular matrix of polymeric substances which gives the bacterial community the shape and a strong adherence power to attach to the surface and to each other. This extracellular matrix of polymeric substances layer also protects the bacterial community from the external challenges, such as antibiotics or the human immune system. Inside this 3D structure, the bacterial community has limited access to nutrients and oxygen, but is better protected from external challenges. As a consequence, bacteria inside the 3D structure exhibit different phenotypic characteristics than the bacteria that form the outer layer of the biofilm. As an example, the bacteria inside the 3D structure are metabolically less active, grow more slowly, and divide less frequently.

Occasionally, newly divided bacteria leave the biofilm. In this dispersal phase, individual bacteria again become motile as they regain flagella (Monroe 2007, O'Toole 2000). During an infection, this dispersal phase can make the conditions worse and spread the infection by constantly making new biofilm. Though the dispersal mechanism is still not clear, it has been reported that the *P. aeruginosa* dispersal phase is controlled by an enzyme called alginate lyase (Boyd 1994). Alginate is an important component of the extracellular matrix in this bacterium. A high level of alginate lyase will decrease the level of alginate; as a result, the extracellular matrix will become thinner, which will increase dispersal of bacteria from the surface. The *algL* gene encodes a protein that controls the production of alginate lyase (Boyd 1994).

2.2 Gene expression during biofilm development

Timely formation of all the organelles that characterize the different stages of biofilm formation requires a strong regulation of gene expression within each bacterium and a strong communication between bacteria. After years of scientific study, we now know that quorum sensing is a very important mechanism for bacteria to communicate with each other and regulate gene expression (Njoroge 2009, Pan 2009). Quorum sensing is a mechanism where certain bacteria secret signaling molecules which are recognized by receptors of another group of bacteria. These receptors are specific for each signaling molecule. Once signaling molecules bind to the receptors, a specific set of genes will be activated. As quorum sensing is only present

in bacterial communities and not in humans, it has been established as a major drug target mechanism for biofilm associated human diseases.

Two-component signal transduction systems (2CSTS) are a response mechanism which directly controls gene expression according to the environmental stress. The RcsCDB system is known to be involved in biofilm formation by regulating the capsule synthesis genes (Gottesman 1985). A large number of 2CSTS were hypothesized to be involved in biofilm formation by a computational study (Denton 2008). By identifying the temporal expression of these 2CSTSs, especially identifying the 2CSTSs involved in the very first stages of biofilm formation, or by identifying the 2CSCTs which are expressed at the outermost layer of the 3D mushroom shaped biofilm, we can go one step towards the establishment of 2CSTSs as a novel prevention and treatment target for the biofilm related infections.

Each 2CSTS is composed of a sensor kinase and a response regulator. Typically, the membrane bound histidine kinase acts as a sensor for the environmental stress. In response to the signal, autophosphorylation occurs at a conserved histidine within the transmitter domain of the sensor kinase. The response regulator receives the phosphate at a conserved aspartate within its N-terminal receiver domain. The response is next transmitted to the C-terminal output domain of the response regulator, which ultimately leads to a protein-protein interaction (flagellar switch) or protein-DNA interaction (regulation of gene expression) (Wolanin 2002). Dephosphorylation of the response regulator occurs to return to the pre-stimulus state (Parkinson 1993).

There are structural and functional exceptions in 2CSTSs. ToxR from *Vibrio cholerae* is a transmembrane sensor that binds specifically to the promoter regions of virulence factor genes through its cytoplasmic domain, resulting in regulation of virulence components for this intestinal pathogen. ToxR is considered a one-component sensory transduction system (Moat 2002). Another exception would be RcsCDB system in *E. coli*. RcsC is a unique membrane hybrid sensor, RcsD is a histidine-containing phosphotransmitter, and RcsB is the transcriptional regulator. This system is considered a three-component sensory transduction or phosphorelay system.

According to the structure and function, most histidine kinases fall into three different groups (Table 2) (Mascher 2006).

Type	**Characteristics**	**Stimulus can sense**
Periplasmic-sensing	• Sensor domain is periplasmic and kinase domain is in the cytoplasm • Sensor domain has at least two transmembrane helices	• Nutrients and solutes.
Cytoplasmic-sensing	• Membrane anchored or soluble proteins are attached to the sensor domain	• Cytoplasmic changes, developmental state of the cell, the cell cycle.
Mechanical stress-sensing	• Highly develop sensor group contains 2-20 transmembrane regions • Missing periplasmic output domain	• Mechanical stress due to some membrane bound compound

Table 2 ***Three major groups of histidine kinases.***

The largest group is the periplasmic sensing histidine kinases. The specialty of this group is that all the histidine kinases have the sensory and the kinase domains, at two different cellular locations. The sensor domain is periplasmic and the kinase domain is in the cytoplasm. The sensor domain has at least two transmembrane helices. As the sensor domain is extracellular, these kinds of histidine kinases sense nutrients and solutes (Mascher 2006). EnvZ (osmolarity sensor) and DcuS (regulator of C4-dicarboxylic acid metabolism) are examples for periplasmic sensing histidine kinases. The second largest group of histidine kinases is the cytoplasmic sensing histidine kinases. This group of the histidine kinase attaches membrane anchored protein or soluble protein in its sensor domain. This kind of kinase senses the presence of cytoplasmic solutes or the developmental state of the cell or the cell cycle (Mascher 2006). ArcB (facultative anaerobic metabolism sensor) and NtrB (nitrate sensor) are cytoplasmic sensing histidine kinases. The third group of histidine kinases consists of highly developed proteins that contain 2-20 transmembrane regions which are imbedded into the membrane; all the transmembrane regions are connected through the intra- or extracellular linkers. This group of histidine kinases doesn't have a periplasmic output domain. As a consequence, this group of histidine kinases senses the stimuli directly associated with the membrane, such as any kind of mechanical stress due to some membrane bound compound. It can also measure the stimuli like ion or electrochemical gradients or transport processes (Mascher 2006).

Different response regulators are also classified in different groups according to their structural and functional diversity (Gao 2007). The division is obtained on the basis of the study of almost 900 response regulators from 400 sequenced bacterial

and archaeal genomes from a genome database (MiST: Microbial Signal Transduction database). Among these response regulators, almost 17% contain isolated receiver domains, which regulate the target either by intermolecular interaction or function as phosphoryl shuttle proteins within phospho-relays (Gao 2007). This group of response regulators doesn't have any separate DNA binding domain. Regulation of flagella by the chemotaxis protein CheY is one example of intermolecular interaction. The remaining response regulators are classified on the basis of the sequence similarity of their effector domains. All these diverse regulatory domains get their active configuration after phosphorylation. OmpR (osmolarity sensor) and NtrC (nitrate sensor) are examples of response regulators with a DNA binding domain (Gao 2007).

2.3 *Escherichia coli* biofilm

A number of research studies have been undertaken to understand gene expression within various bacterial biofilms, such as those caused by *E. coli, P. aeruginosa* and *Vibrio cholera* (Danese 2000, Mikkelsen 2011). *E. coli* is considered a model organism, as it is the most studied organism in lab. It is a gram-negative enterobacterium. The species of *E. coli* has many different strains. Most of these are non-pathogenic, but some strains like *Escherichia coli* O157:H7 are pathogenic and responsible for food poisoning in humans. Usually, non-pathogenic *E. coli* strains are found in our normal intestinal flora to help the body produce vitamin K_{12} and prevent other pathogenic microorganisms from colonizing the intestine. *E. coli* is a non-spore forming facultative anaerobic bacteria approximately 2 micrometers (μm) in length

and 0.5 μm diameter. The optimal growth temperature for *E. coli* is 37 °C. Most of the *E. coli* strains are motile due to their flagellar movement. *E. coli* is also a good biofilm former. The thickness of an *E. coli* biofilm could be 200 to 300 μm.

In *E. coli,* some 2CSTSs like the colanic acid activator system RcsCDB (Stout 1990) and the osmoregulation system EnvZ/OmpR (Combaret 2001) have a strong effect on biofilm formation. Colanic acid is a very important extracellular matrix component for biofilm formation. The colanic acid mutant strains of *E. coli* are not able to form three dimensional mushroom-shaped structured biofilm (Danese 2000). Colanic acid production in *E. coli* is regulated by the RcsCDB phosphorelay system (Stout 1990), where RcsC acts as a membrane-bound sensor kinase and RcsB is the response regulator. The environmental stress is sensed by the kinase domain of RcsC and transmitted to the receiver domain of RcsC. The phosphorylation of RcsC leads to the transfer of the environmental stress signal through the phosphate group to the RcsB response regulator via histidine-containing phosphotransmitter domain protein, RcsD (Charlot 2005, Ferrières 2003). After phosphorylation, RcsB transcriptionally regulates the *cps* genes, which are required for capsule synthesis.

The osmoregulator 2CSTS OmpR-EnvZ has an important role to help *E. coli* adapt to changes of extracellular osmolarity by inversely regulating two major outer membrane protein encoding genes, *ompC* and *ompF* (Ferrières 2003). OmpC is expressed at high osmolarity and OmpF is expressed at low osmolarity. EnvZ is a membrane-bound sensor kinase and OmpR is the corresponding response regulator. At high osmolarity, the phosphorylation level of OmpR increases, which consequently

represses the expression of OmpF and activates the expression of OmpC. In low osmolarity, the expression of OmpF is activated and the expression of OmpC is repressed as a result of a decreased level of phosphorylation of OmpR. After phosphorylation, OmpR also up-regulates *csgD* which encodes a transcription activator of the *csgBA* operon. CsgB and CsgA are the major curli subunits (Brombacher 2003). Curli are very important cell surface organelles, normally found in the irreversible attachment stage of biofilm formation, which helps bacteria to attach to the surface very tightly.

DcuS is a typical periplasmic sensing histidine kinase. It has a membrane bound histidine kinase with four β-stands, surrounded by α-helices and a cytoplasmic kinase domain. DcuSR regulates two important operons, *frdABCD* and *dcuB* for anaerobic growth of *E. coli,* using C_4-dicarboxylates as substrates (Zientz 1998, Golby 1999). To use C_4-dicarboxylates (aspartate, malate, fumarate and succinate) as substrates, *E. coli* needs to synthesize fumarate reductase and the fumarate/succinate antiporter. The succinate antiporter in *E. coli* body is encoded by *dcuB* and the *frdABCD* operon encodes the four subunits of fumarate reductase (Janausch 2002, Krämer 2007, Golby 1999). In a computational study from our lab (Denton 2008), we hypothesized that DcuSR may be involved in biofilm formation, a hypothesis that will be tested in this thesis.

In *E. coli,* beside 2CSTS, the global transcriptional regulator FlhD/FlhC has an effect on biofilm formation. Physiological experiments from our lab established that FlhC reduced the cell division rate and the amount of biofilm (Sule 2011). FlhD/FlhC

originally was described as a regulator of flagella synthesis in *E. coli* (Bartlett 1988). The later discovered repression of aerobic respiratory genes by FlhD/FlhC, accompanied by an induction of the anaerobic respiratory genes (Prüβ 2003), implies that FlhD/FlhC may participate in the switch from aerobic to anaerobic growth that occurs as bacteria transition from the free living environment to the human host. The *flhD* operon is regulated by both EnvZ/OmpR and RcsCDB. In their phosphorylated form, both of the response regulators down-regulate *flhD* expression (Shin 1995, Francez-Charlot 2003). Flagella aid biofilm formation during reversible attachment and dispersal. During irreversible attachment and maturation, bacteria lose their motility because at that time they don't synthesize flagella. Controlling flagella synthesis according to the developmental stages during biofilm formation is mediated by FlhD/FlhC.

2.4 Fluorescence microscopy to study gene expression in biofilms

Most of the previous studies on biofilm formation have been performed to determine the temporal expression of different 2CSTSs at different developmental stages. We have a very limited knowledge about the spatial expression of those 2CSTSs within the 3D biofilm structures. In this study, we are focusing on the spatial expression of selected 2CSTSs, as well as FlhD/FlhC. We are using the green fluorescence protein (GFP) and red fluorescence protein (RFP) as reporter genes. Selected promoters were fused in front of the open reading frame of GFP and RFP and the expression of fluorescence was observed using fluorescence microscopy. In this microscopy, a specific single wavelength first excites the sample atoms. As a result of

this excitation, the electrons jump to a higher energy level. When the electrons drop back to the ground state, after emitting the photon, the sample gives the fluorescence signal at a higher wavelength than the excitation wavelength. Using that particular emitting wavelength, fluorescence microscopy can detect the signal of the sample. Fig-3 is a schematic diagram of fluorescence microscopy. In fluorescence microscopy, two filters are used, an excitation filter and an emission filter. The excitation filter converts the light source into a single wavelength monochromatic light and the emission filter blocks the excitation light source from reaching the detector. Most of the fluorescence microscopes used in biological fields are epifluorescence microscopes. In this type of fluorescence microscope, monochromatic excitation light passes through the objective lenses to the specimen from above (in case of upright microscope) or from bellow

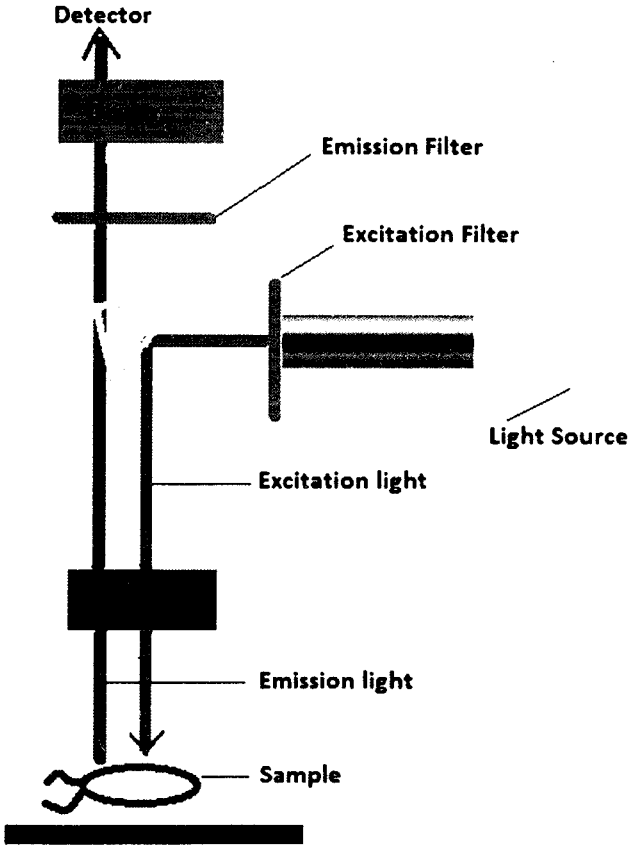

Fig - 3 ***Schematic diagram of fluorescence microscopy.*** *Particular wavelength excitation light after passes through the objective lenses excite the fluorescence sample and the emitted light from that sample passes through the emittion filter and ocular. At last the emittion light can be detected through the detector.*

(in case of inverted microscope). In this microscope setup, most of the excitation light passes through the objective lenses and only a small amount of the reflected excitation light can reach the objective lenses along with the emitted light. As a result, the background noise is less when compared to the actual signal. Sometimes an extra lens is used to block the reflected excitation light giving an even better signal to noise ratio.

In modern biofilm research, fluorescence microscopy is a very powerful tool. Fluorescence microscopy is widely used to detect and quantify the microorganisms in a sample using fluorescence *in situ* hybridization (FISH) with rRNA-targeted oligonucleotide probes. Previously using FISH, the cellular content of ribosomes has been quantified in relationship to the growth rate of single cells of a specific population of bacteria in multispecies anaerobic biofilms (Poulsen 1993). Recently, fluorescence microscopy has been used widely to study the different timescales of biofilm development (hours to days) in 3D structure (Bridier A 2011), as well as the high-density microarray platform consisting of nano-biofilms of *Candida albicans* (Srinivasan 2011). Using advanced computer software, we can reconstruct a virtual 3D image by assembling z-stack images. Z- stacks is a program which can move the focal point of the objective lens through the Z-axis of a sample. While moving, microscope can take several images of any point along the Z-axis of a sample. Then the focused images can be accumulated into one image and the unfocused images can be discarded. As a result we get a very sharp and clear final image.

For this study, we are using a Zeiss Axio Observer Z1 inverted fluorescence microscope. This is also an epifluorescence microscope with the ability to take the Z-stack images. This microscope has extremely low light scattering power as a result of high contrast. Using this fluorescence microscope, primarily all newly transformed bacterial strains containing the selected promoter fused GFP plasmids were tested and we got signals. A number of troubleshooting modifications were made for real-time fluorescence microscopic experiments, but in future, more technical problems well need to be solved before we get reliable data from this experiment.

MATERIALS AND METHODS

1. Bacterial Strains

The strains we used for the SEM experiment were AJW678 (kindly provided by Alan J. Wolfe, Loyola University Chicago, Maywood, IL) as a parental strain and its isogenic *ackA* mutant and *ackA pta, ackA ompR, ackA rcsB, ackA dcuR* double mutants (Table 3, strains 1 through 9). For the fluorescence microscopy experiment, we purchased an *E. coli* promoter collection (Cat# PEC3877) from Open Biosystems, Thermo Scientific (Huntsville, AL). This promoter collection includes 1931 promoters (out of 2500 promoters in the entire genome) for the *E. coli* K12 strain MG1655, fused to the open reading frame of GFP (*gfpmut2*) on pUA66 and pUA139 vectors (Zaslaver 2006). GFP fusions to the *ackA*, *dcuR*, *ompR*, and *ompC* promoters were used in this project from this collection (Table 3, strains 11 through 14). Since the collection was lacking the *flhD* promoter fusion, we constructed fusions of several *flhD* promoter fragments. An additional *ompR* promoter fusion was constructed to see the differences of expression level from the same promoter in two different vectors. We used both AJW678 and MC1000 (Table 3, strain 10) as sources for the *flhD* and *ompR* promoter fragments. Though the *ompR* promoter regions of both strains are identical, MC1000 has a longer *flhD* promoter region than AJW678 due to an insertion sequence-5 (IS5) in MC1000. Because of the IS5 element, MC1000 is more motile than AJW678 (Barker 2004). And finally, AJW678 was transformed with all of these GFP fused promoter plasmids (Table 3, strains 15 through 20 and corresponding

plasmids). The cloning procedure for the strains and plasmids will be outlined in chapter 4.2.

		Relevant genotypes	Reference
#		**Strains**	
1	AJW678	*thi-1 thr-1*(am) *leuB6 metF159*(Am) *rpsL136 ΔlaxX74*	Kumari et al. 2000
2	AJW1939	AJW678 *ackA*::kn	Kumari et al. 2000
3	AJW2013	AJW678 Δ(*ackA pta hisJ hisP dhu*) *zej*223-Tn10	Wolfe et al. 2003
4	AJW2050	AJW678 *ompR*::Tn10	Alan J. Wolfe
5	AJW2143	AJW678 *rcsB*::Tn5	Fredericks et al. 2006
6	AJW2147	AJW678 *rcsB*::Tn5 *ackA*::Tn*phoA'*-2	Fredericks et al. 2006
7	BP1286	AJW678 *dcuR*::kn	CGSC, Prüß et al. 2010
8	BP1318	AJW678 *ackA*::Tn*phoA'*-2 *dcuR*::kn	Prüß et al. 2010
9	BP1291	AJW678 *ackA*::kn *ompR*::Tn10	Prüß et al. 2010
10	MC1000	F-, *k-*, *araD139 Δ(araAB-leu)7,696 Δ(lacIY)74 galU galK rpsL thi*	Casadaban and Cohen (1980)
11	BP1429	AJW678 pU66 - p*ackA*	This study
12	BP1430	AJW678 pU139 - p*dcuR*	This study
13	BP1431	AJW678 pU139 - p*ompR*	This study
14	BP1432	AJW678 pU139 - p*ompC*	This study
15	BP1399	AJW678 pPS29	This study
16	BP1402	AJW678 pPS36	This study
17	BP1414	AJW678 pPS43	This study
18	BP1411	AJW678 pPS50	This study
19	BP1420	AJW678 pPS55	This study
20	BP1417	AJW678 pPS62	This study

#	Plasmids		
1		pU66 - p*ackA*	Open Biosystems
2		pU139 - p*dcuR*	Open Biosystems
3		pU139 - p*ompR*	Open Biosystems
4		pU139 - p*ompC*	Open Biosystems
5	pGEM-T Easy	General cloning vector for PCR-amplified products	Promega
6	pAcGFP1-1	Green fluorescence tagged cloning vector	Clontech
7	pDsRed2-1	Red fluorescence tagged cloning vector	Clontech
8	pPS1	pGEM-T Easy - p$flhD_{AJW678}$	This study
9	pPS8	pGEM-T Easy - p$flhD_{MC1000}$	This study
10	pPS23	pGEM-T Easy - p$ompR_{MC1000}$	This study
11	pPS29	pAcGFP - p$flhD_{MC1000}$	This study
12	pPS36	pDsRed - p$flhD_{MC1000}$	This study
13	pPS43	pAcGFP - p$ompR_{MC1000}$	This study
14	pPS50	pDsRed - p$ompR_{MC1000}$	This study
15	pPS55	pDsRed - p$flhD_{AJW678}$	This study
16	pPS62	pAcGFP - p$flhD_{AJW678}$	This study

Table 3 ***Bacterial strains and plasmids used in this study.***
*The kanamycin resistance (*AJW2143*) and the tetracycline resistance (*AJW2013, AJW2050, BP1291*) of the above strains are due to the transposons Tn5 and Tn10, respectively, and kn is an insertion of the kanamycin resistance gene. Δ refers to a deletion of the respective gene. The TnphoA transposon also confers resistance towards tetracycline.*

2. Growth Conditions

Bacterial strains were stored at -80°C in 10% dimethyl sufoxide (DMSO). Before using, the bacterial strains were streaked on Luria Bertani (LB, 1% tryptone, 0.5% yeast extract, 0.5% NaCl, 1.5% agar) plates and incubated overnight at 37°C. From the

plate, the bacterial cultures were inoculated into liquid LB media (in case of electron microscopy experiment) or into liquid tryptone broth (TB, 1% tryptone, 0.5% NaCl) (in case of fluorescence microscopy experiment) and grown overnight at 37°C. According to the resistance markers on some of the strains (Table 3), antibiotics were added to the overnight cultures and the plates.

3. Biofilms Under SEM

3.1. Growth of the bacterial biofilm

Overnight cultures of the parental *E. coli* strain and the isogenic mutant strains were diluted 100 fold in 4 ml of fresh LB broth in six-well plates and incubated at 32°C for 48 hours. Before inoculation, we put one 12-mm glass cover slip in each well. As a result, the biofilms formed on the glass cover slips, as well as on the surface of the liquid media. We preserved and analyzed both biofilms by removing the liquid carefully and washing each well with phosphate buffered saline (PBS) twice.

3.2. Preparation of the biofilm for SEM

Washed biofilms were air-dried and fixed using 2 ml of 2.5% glutaraldehyde (Tousimis Research Corporation, Rockville MD) in 0.1 mol l^{-1}sodium phosphate buffer. After 2 hours of fixation at 4°C, the biofilms were dehydrated with graded alcohol series treatment and then critical point dried. For the graded alcohol series, biofilm samples were treated for 15 minutes each in 30%, 50%, 70%, and 90% ethanol and finally with 100% ethanol for 15 minutes twice (Sule et al. 2009, Prüβ et al. 2010). For the critical point drying, liquid carbon dioxide was used in an Autosamdri-810 critical point drier (Tousimis Research Corporation, Rockville MD). Once the dehydration of

the biofilms was done, the glass cover slips were attached to aluminum mounts with adhesive silver paint. Lastly, the slips were coated with gold-palladium using a Balzers SCK 030 sputter coater (Sule et al. 2009).

3.3. SEM

The images of the biofilms were obtained using a JEOL JSM-6490LV scanning electron microscope (JEOL Ltd., Japan). For each strain and experiment, we produced 5 to 6 images at different magnifications (1000X, 3000X and 6500X). The experiment was repeated three or four times for each bacterial strain to a total of at least 15 to 24 images per strain. One representative SEM image of each bacterial strain at 3000X magnification is included in the Results. Biofilms produced by each strain were largely consistent throughout all images.

4. Fluorescence Microscopy Experiment

To study the temporal expression from selected promoters during biofilm formation, we purchased the *E. coli* promoter collection from Open Biosystems. The missing promoter *flhD* along with another promoter of an important regulator *ompR* were fused to the open reading frames of pAcGFP1-1 or pDsRed2-1 plasmids. AJW678 was transformed with the resulting plasmids. Expression of the fluorescence proteins was visualized with fluorescence microscopy.

Once our strains were ready, we studied the temporal expression from the *ompR*, *flhD*, *flhC*, *ackA*, and *dcuR* promoters in planktonic cultures, using the 96-well plate assay. We also tested the newly constructed strains under the fluorescence microscope to see their signals.

4.1 Promoter collection

We purchased GFP fused *E. coli* promoters from Open Biosystems as part of their *E. coli* promoter collection. This promoter collection includes 1931 promoters (out of 2500 promoters in the entire genome) for *E. coli* K12 strain MG1655 fused to GPF (*gfpmut2*) on pUA66 and pUA139 vectors (Zaslaver 2006). Vectors pUA66 and pUA139 are mostly identical, except the restriction sites BamHI and XhoI are reversed. pUA66 was used to clone the promoter region of genes expressed on the positive strand, whereas pUA139 was used to clone the promoter region of genes expressed on the negative strand. The promoter fragments were obtained from MG1655.

Strains that were transformed with these vectors that contained the *ackA*, *dcuR*, *ompR*, and *ompC* promoter fusions were retrieved from the collection by growing them on LB + kanamycin (25 μg/ml) plates at 37°C overnight. From the plates, the bacterial cultures were inoculated into liquid LB + kan (25 μg/ml) media and incubated overnight at 37°C. Vectors were purified using Wizard® Plus SV Minipreps DNA Purification kits (Promega, Madison WI). At last, AJW678 was transformed with these isolated plasmids (plasmid # 1-4 from Table 3). After transformation, the bacterial strains (strain # 11-14 from Table 3) were stored at -80°C.

4.2 Cloning

Figure-4 shows the steps to clone promoter fused pAcGFP1-1 or pDsRed2-1.

A. ***Primer design and PCR:*** As a first step, we designed the primers for the *ompR* and *flhD* promoter regions using Integrated DNA Technology SciTools from www.idtdna.com. The promoter regions of both *ompR* and

flhD were amplified by polymerase chain reaction (PCR) using primer # 1 and 2 (for *flhD*) and primer # 3 and 4 (for *ompR*) from Table 4.

#	Name	Sequence(5'-3')	Tm	%GC
1	*flhD*-promo5'	AGATCTTGACTGTGCGCAACATCCCATT	74.9	46.43
2	*flhD*-promo3'	GGTACCTGCCAGCTTAACCATTTGCGGA	76.6	53.57
3	*ompR*-promo5'	AGATCTGTCGATTTCACGCAGACGCTTT	74.2	46.43
4	*ompR*-promo3'	GGTACCTGTCGTCATCGACCACCAGAAT	74.5	53.57
5	GFP/RFP- 5'	CTGTGGATAACCGTATTACCGCCA	69.1	50.00
6	GFP-3'	TGAACTTGTGGCCATTCACATCGC	73.7	50.00
7	RFP-3'	ATGAACTCGGTGATGACGTTCTCG	70.3	50.00

Table 4 ***List of the primers used in this study***.

5' primers are forward primers and 3' primers are reverse primers. Primer # 1-4 were used to amplify the ompR and flhD promoters from E. coli strains AJW678 and MC1000, and primer # 5-7 were used to sequence the cloned fragments.

PCR: For PCR, we used the following amplification program :

1. Initialization temperature of 94°C for 5 minutes
2. Denaturation temperature of 94°C for 1 minute
3. Annealing temperature of 60°C for 30 seconds
4. Elongation temperature of 72°C for 3 minutes
5. Go to step 2 (30 times)
6. Final elongation temperature of 72°C for 7 minutes
7. Final holding temperature at 4°C (indefinite time)

B. ***Cleaning of the fragments***: After the PCR was done, the amplified *ompR* and *flhD* promoter fragments were separated on a 0.8% low-melting point agarose gel. The amplified DNA fragments were recovered from the gel using the Wizard® SV Gel and PCR Clean-Up System (Promega, Madison WI).

C. ***Ligation and transformation***: The recovered PCR products were ligated into pGEM-T Easy (Promega, Madison WI) which carries *lacZα*, a truncated form of the gene that encodes β-galactosidase and permits α-complementation and blue/white selection. Commercially competent JM109 cells that were provided with the pGEM®-T Easy Vector System kit were then transformed with the ligated pGEM-T easy vectors. For the transformation, we used a 1:100 volume of DNA to competent cells and kept the mixture on ice for 20 minutes. We then heat shocked the mixture in a hot water bath at 42°C for 2 minutes to allow the vectors to penetrate the bacteria. Transformed bacteria were put on ice for 1 minute and then incubated at 32°C for 3 hours into Super Optimal broth with Catabolite repression (SOC; 2% w/v bacto-tryptone, 0.5% w/v bacto-yeast extract, 10mM NaCl, 2.5mM KCl, 10mM $MgCl_2$, 20mM glucose).

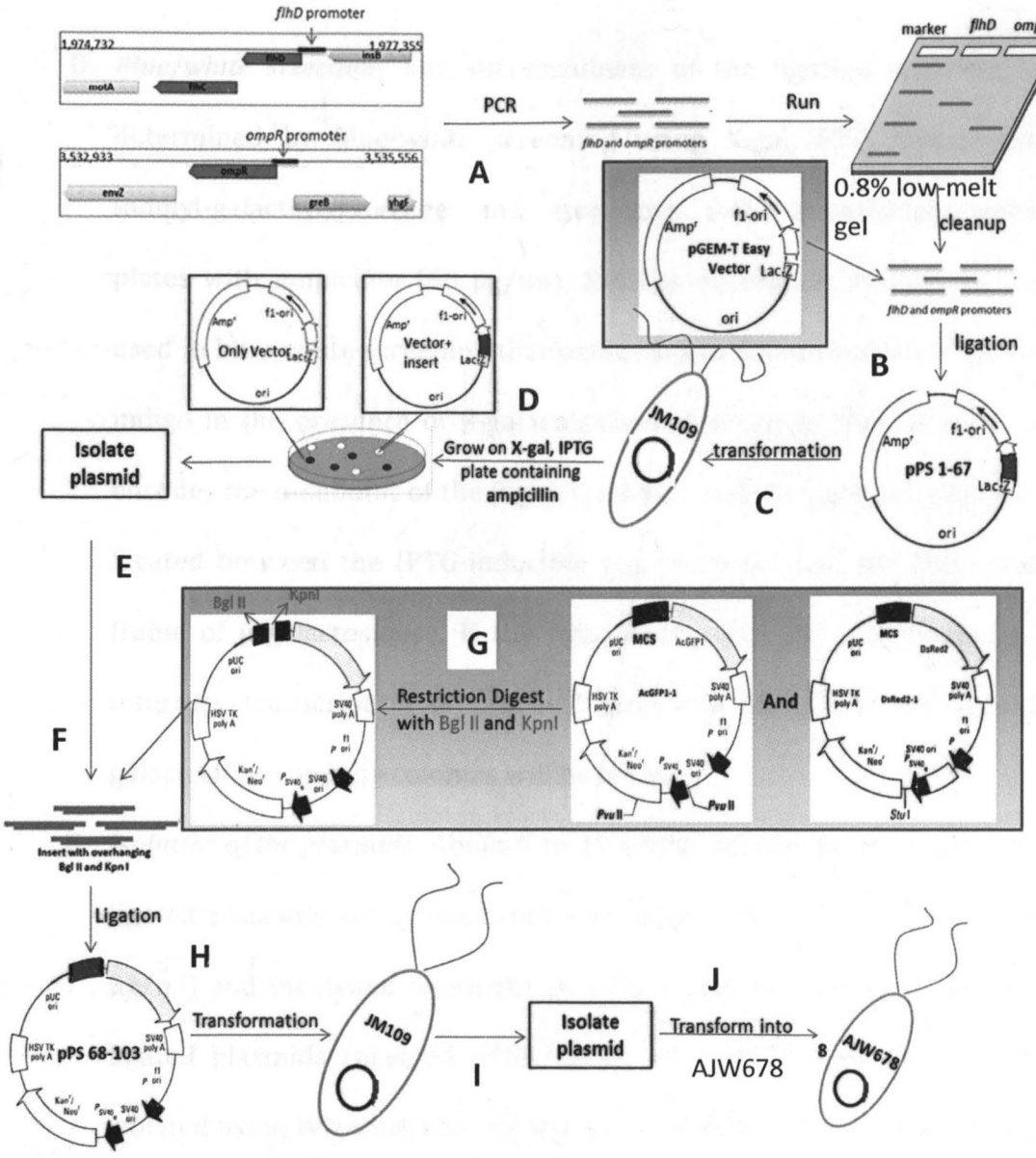

Fig - 4 ***Steps of cloning.***

ompR and flhD promoter regions were cloned into AcGFP1-1 and DsRed2-1. Promoter regions were first ligated into pGEM-T Easy vector and transformed into JM109. The resulting plasmids were digested with KpnI and BglII and ligated into AcGFP1-1 and DsRed2-1 plasmids that had been digested with the same enzymes. First JM109 and then AJW678 competent cells were transformed with the promoter fused AcGFP1-1 and DsRed2-1. Bold capital letters indicate the individual cloning steps that are consistent with the description in the text.

D. ***Blue/white selection:*** The successfulness of the ligation reactions were determined by blue-white screening using X-gal/IPTG (bromo-chloro-indolyl-galactopyranoside and isopropyl β-D-1-thiogalactopyranoside) plates with ampicillin (50 μg/ml). X-gal is an organic compound widely used in blue-white screening that oxidizes into 5,5'-dibromo-4,4'-dichloro-indigo in the presence of β-galactosidase to produce blue colonies. *lacZ* encodes the α-subunit of the β-galactosidase and multiple cloning sites are located between the IPTG-inducible p_{tac} promoter and the open reading frame of β-galactosidase. If the ligation is successful, the fragment will interrupt transcription of the *lacZ* gene and there will not be any β-galactosidase and the colonies will be white.

E. ***Isolation of the plasmids:*** About 5 to 10 white colonies for each of the three ligated plasmids were inoculated into liquid LB + Ampicillin media (50 μg/ml) and incubated overnight at 37°C. Using the overnight culture, the ligated plasmids (plasmid pPS1, pPS8, and pPS23 from Table 3) were isolated using Wizard® Plus SV Minipreps DNA Purification kits (Promega, Madison WI).

F. ***Restriction digests of the pGEM derivative plasmids:*** One plasmid with each of the $flhD_{AJW678}$ and $ompR_{MC1000}$ promoters (pPS1and pPS23, respectively) were digested with BglII (A'GATCT) and KpnI (GGTAC'C) to recover the promoter regions. In the case of the plasmid that contained the $flhD_{MC1000}$ promoter (pPS8), we used EcoRI (G'AATTC) and KpnI (GGTAC'C) for digest.

After the restriction digests, the mixtures were separated on 0.8% low-melting point agarose gels. The *flhD*$_{MC1000}$, *flhD*$_{AJW678}$ and *ompR*$_{MC1000}$ promoters were recovered and cleaned with the Wizard® SV Gel and PCR Clean-Up System (Promega, Madison WI).

G. ***Restriction digest of the GFP and RFP plasmids:*** We also digested the pAcGFP1-1 and pDsRed2-1 plasmids with BglII – KpnI and EcoRI – KpnI and cleaned them with the Wizard® SV Gel and PCR Clean-Up System from the 0.8% low-melting point agarose gels. The 5′-phosphate groups of the digested pAcGFP1-1 and pDsRed2-1 plasmids were then hydrolyzed by Calf Intestinal Alkaline Phosphatase (CIAP, Promega, Madison WI). CIAP catalyzes the hydrolysis of 5′-phosphate groups from DNA or RNA. The CIAP reaction prevents the religation of the digested pAcGFP1-1 and pDsRed2-1 plasmids during the ligation reaction. After the CIAP reaction, the pAcGFP1-1 and pDsRed2-1 plasmids were recovered from the CIAP reaction mixture using Phenol/chloroform extraction and ethanol precipitation, as recommended by the manufacturer of the CIAP reagents. For the phenol/chloroform extraction, we used an equal volume of the phenol/chloroform mixture to the CIAP reaction solution. After 1 minute of vortexing, the samples were centrifuged at 15000 rpm for 5 minutes and the aqueous layer was transferred to a new tube. To remove traces of phenol, an equal volume of chloroform was added to the aqueous layer and centrifuged at 15000 rpm for 5 minutes. After that, we transferred the

aqueous layer into a new tube and finally the purified DNA was collected by ethanol precipitation at -20°C overnight.

H. ***Ligation and transformation into JM109:*** The *flhD*$_{MC1000}$, *flhD*$_{AJW678}$ and *ompR*$_{MC1000}$ promoters were ligated into digested and CIAP-treated pAcGFP1-1 and pDsRed2-1 plasmids. The JM109 competent cells (Promega, Madison WI) were transformed with the freshly ligated plasmids (plasmid pPS29, pPS36, pPS43, pPS50, pPS55, pPS62 from Table-3), using ampicillin as selective marker on the agar plates.

I. ***Isolation of the promoter fusion plasmids:*** Four transformants from each of the six with promoter-fused pAcGFP1-1 or pDsRed2-1 plasmids were inoculated into liquid LB + Kan and incubated overnight at 37°C. Using that overnight culture, the plasmids were isolated using Wizard® Plus SV Minipreps DNA Purification kits. The promoter regions of all four isolated plasmids from each of the six transformations were sequenced at Macrogen USA (Rockville MD), using primer # 5-7 from Table-4; primer # 5 was used as a forward primer for all plasmids, whereas primer # 6 and 7 were used as reverse primers for GFP and RFP plasmids, respectively. The PCR amplified *ompR*$_{MC1000}$, *flhD*$_{MC1000}$ and *flhD*$_{AJW678}$ promoters (from step A) were also sequenced at Macrogen USA using primer # 1-4 from Table-3. This was done as a positive control for the cloned promoters.

J. ***Transformation into AJW678:*** pPS29, pPS36, pPS43, pSP50, pPS55, and pPS62 were selected for final transformation into chemically competent

AJW678. The new strains (BP1399, BP1402, BP1414, BP1411, BP1420, and BP1417 from Table-3) were stored at -80°C.

4.3 96-well microtiter plate assay

A 96-well plate assay was performed to determine temporal expression from the respective promoters in planktonic bacteria. All newly constructed strains (strain # 11 – 20 from table-3) were first grown on the LB plates overnight at 37°C. Antibiotics were added to the plate as required. From the plates, bacterial strains that were newly constructed (strain # 15- 20 from table-3) were inoculated into liquid TB + Kan (50 μg/ml) and those strains that were obtained from the collection (strain # 11-14 from table-3) were inoculated into liquid TB + Kan (25 μg/ml) overnight at 37°C. Overnight cultures were diluted 100 fold in 200 μl of fresh TB into individual wells of 96-well plates that had clear bottoms to permit fluorescence readings and black walls to avoid cross signaling (Greiner Bio-One, Germany). Plates were incubated at 32°C for a maximum of 7 days. Each row of the 96-well plates was inoculated with one bacterial strain at different time points. Each strain was inoculated into six wells from one line. Once the incubation was done, the fluorescence intensities were quantified using a Synergy HT Multidetection Fluorescence Capability Microplate Reader (BioTek, Winooski, VT). The fluorescence intensity is indicative of expression from the respective promoter. The fluorescence intensity was measured and analyzed to determine temporal expression from the respective promoters.

4.4 Fluorescence microscopy

Initial fluorescence microscopy was performed with biofilms formed by the newly constructed bacterial strains (strain # 11--13 and 17-20 from Table-3).

4.4.1 Growth of the bacterial biofilm

The three newly constructed bacterial strains that contained the promoter::GFP fusions, as well as the four promoter fusions from the collection were grown on LB plates (appropriate antibiotic was added) overnight at 37°C. From the plates, the strains were inoculated into liquid LB (appropriate antibiotic was added) overnight at 37°C. The overnight cultures were diluted 100 fold into 4 ml of fresh LB in 6-well plates and incubated for 2 days at 37°C. Prior to the incubation, one 22-mm sterile square coverslip (VWR, USA) was added to each individual well. After 2 days of incubation, the biofilms on the cover slips were washed twice with PBS.

4.4.2 Biofilm fixation

The biofilms were fixed onto the slips by three different techniques (heat fixation, air fixation and glutaraldehyde fixation) to compare with the unfixed control samples. For heat fixation, the coverslip was loaded onto a microscopy slide and pulled through the flame of a Bunsen burner three times. For air fixation, the biofilms on the slip were kept in the air for 5 minutes. For glutaraldehyde fixation, the slips with the biofilms were treated with 2.5% glutaraldehyde (Tousimis Research Corporation, Rockville MD) in 0.1 mol l^{-1} sodium phosphate buffer for 5 minutes.

4.4.3 Experiment

The biofilm-containing coverslips were observed under a Zeiss Axio Observer Z1 inverted fluorescence microscope using Zeiss FITC filter set 38 HE. The samples were excited for 400 ms (milli-seconds) at 470/40 wavelength. Emission was determined at 525/50 wavelength. For each experiment, 3-4 images were taken at 100X magnification. The experiment was repeated 3 or 4 times for each bacterial strain which produced 9 to 16 images per strain. One representative 100X magnification image of each bacterial strain is shown in the Results.

RESULTS

1. Biofilms under SEM

From a previous high-throughput quantitative biofilm experiment and the phenotype microarray experiment in our lab, we hypothesized that the acetate metabolism mutant strains may form different biofilms than their isogenic parental strain. To confirm this hypothesis and to determine whether any differences between the parental strain and the acetate mutants may depend on 2CSTS response regulators, we performed SEM with biofilms formed by the AJW678 strain and its *ackA* and *ackA pta* mutants (acetate metabolism mutants), as well as double mutants in *ackA* and either of the response regulator genes *ompR, rcsB, or dcuR.* The parental *E. coli* strain exhibited a small number of bacteria homogenously distributed over the coverslip without any clustering (Fig-5, top image). In contrast, the biofilms formed by the *ackA* (second row, left image) and *ackA pta* (second row, right image) mutants have more bacteria. In addition, bacteria form three-dimensional clusters. The biofilm of the double mutant *ackA rcsB* (third row, left image) is structurally different from the *ackA* mutant. Biofilms of this mutant lack the clusters of bacteria; however, the number of bacteria is similar, as compared to the *ackA* mutant. Intriguingly, in the case of the biofilms that are formed by the *ackA dcuR* mutant (third row, right image), bacteria still form three-dimensional clusters, but significantly fewer bacteria form the biofilm than for the *ackA* mutant.

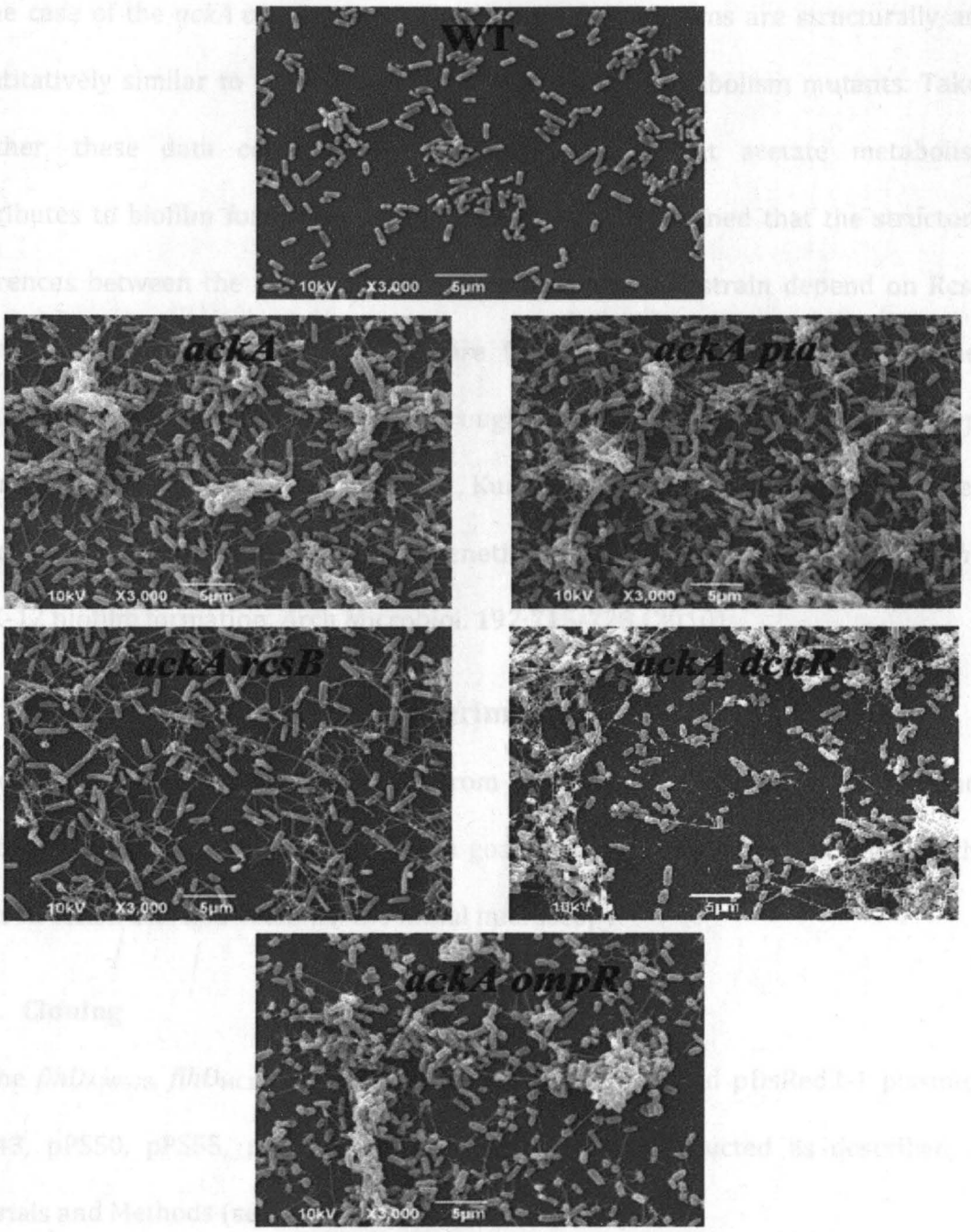

Fig - 5 ***SEM analysis of biofilms formed by the parental E. coli strain and ackA, ackA pta, ackA rcsB, ackA dcuR, and ackA ompR mutants.***

Biofilms were grown in LB for 48 h at 32˚C from AJW678 bacteria and isogenic ackA, ackA pta, ackA rcsB, ackA dcuR, and ackA ompR mutants. Up to 24 scanning electron micrographs were obtained at three different magnifications. One representative image at 3,000 fold magnification is shown.

In the case of the *ackA ompR* mutant (bottom image), biofilms are structurally and quantitatively similar to the *ackA* and *ackA pta* acetate metabolism mutants. Taken together, these data confirm the initial hypothesis that acetate metabolism contributes to biofilm formation. In addition, it was determined that the structural differences between the *ackA* mutant and its parent *E. coli* strain depend on RcsB, while the quantitative differences require DcuR. These findings were published together with the quantitative high-throughput experiment and the phenotype experiment in Prüß, Verma, Samanta, Sule, Kumar, Wu, Christianson, Horne, Stafslien, Wolfe, and Denton, Environmental and genetic factors that contribute to *Escherichia coli* K-12 biofilm formation. Arch Microbiol. 192:715-728 (2010).

2. Fluorescence Microscopy Experiment

To study the temporal expression from selected promoters, the fluorescence microscopy experiment was performed. A goal of this MS thesis was to clone all the required constructs and establish the initial microscopy.

2.1. Cloning

The $flhD_{AJW678}$, $flhD_{MC1000}$, $ompR_{MC1000}$ fused pAcGFP1-1 and pDsRed2-1 plasmids (pPS43, pPS50, pPS55, pPS62, pPS29, pPS36) were constructed as described in Materials and Methods (section 4.2-I).

2.1.1. Gel electrophoresis and the plasmid map

To confirm the size of the promoter insertions within the constructed plasmids, we digested the plasmids with BglII and KpnI (pPS43, pPS50, pPS55, pPS62) or with EcoRI and KpnI (pPS29, pPS36) and separated the restriction

fragments on a 1% agarose gel for 1 hour. We used 1% EZ-Vison loading buffer (VWR, USA). Fig-6 is showing the gel electrophoresis results of the digested plasmids.

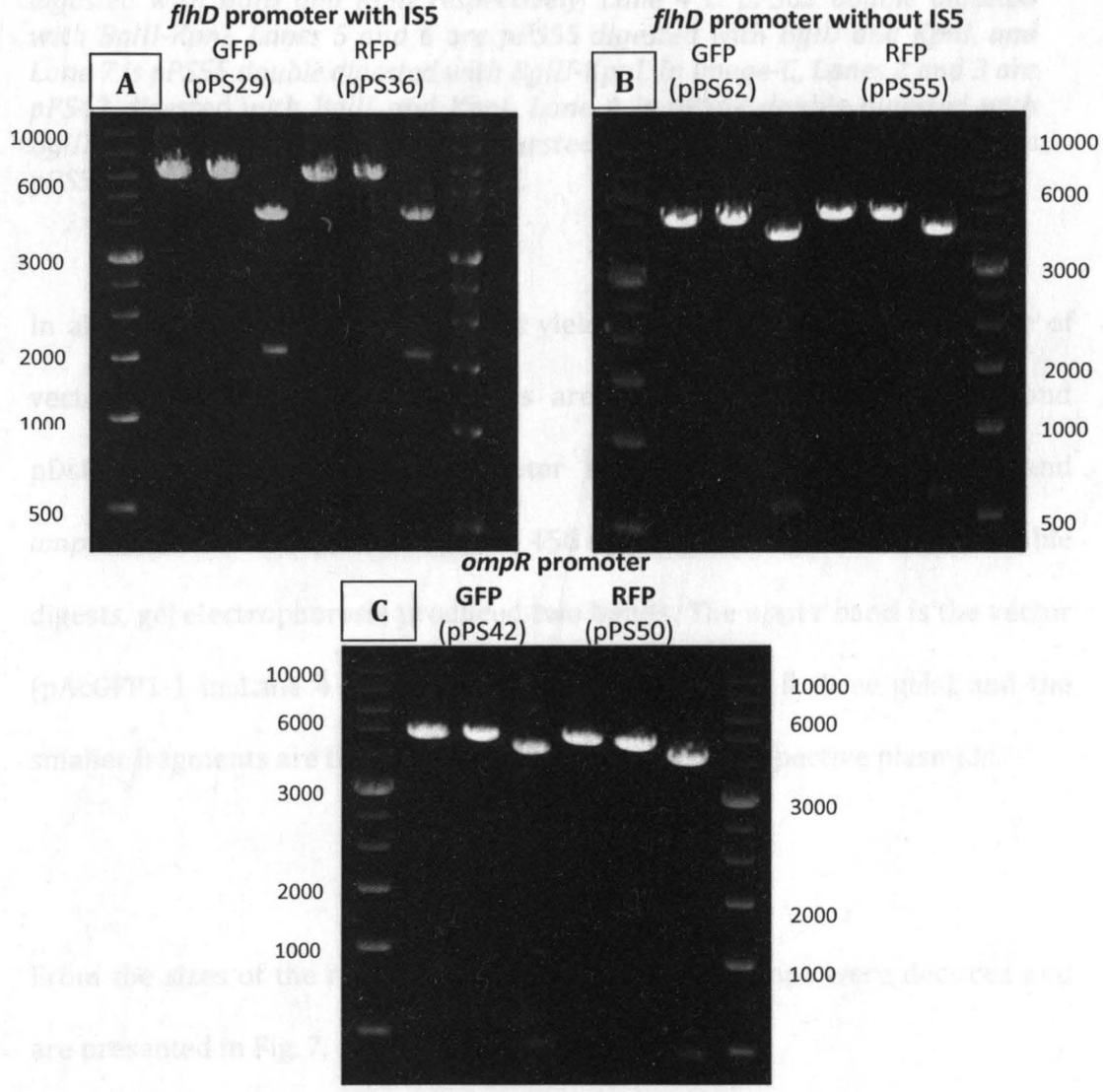

Fig - 6 ***Gel electrophoresis of single and double digested plasmids.***

For all three electrophoretic gels, Lane 1 and 8 contain the 1Kb ladder (Amresco, USA), lane 2, 3, 5 and 6 are the single digested plasmids and lane 4 and 7 are double digested plasmids. The upper left image (A) shows the digested fragments of pPS29 and pPS36 ($flhD_{MC1000}$::GFP and $flhD_{MC1000}$::RFP, respectively). The upper right image (B) is showing the digests of pPS62 and pPS55 ($flhD_{AJW678}$::GFP and $flhD_{AJW678}$::RFP, respectively). The bottom image

(C) is showing the digests of pPS43 and pPS50 (ompR$_{MC1000}$::GFP and ompR$_{MC1000}$::RFP, respectively).

In image-A, Lane 2 is pPS29 digested with EcoRI, Lane 3 is pPS29 digested with KpnI, Lane 4 is pPS29 double digested with EcoRI-KpnI, Lane 5 is pPS36 digested with EcoRI, Lane 6 is pPS36 digested with KpnI, and Lane 7 is pPS36 double digested with EcoRI-KpnI. In image-B, Lanes 2 and 3 are pPS62 digested with BglII and KpnI respectively, Lane 4 is pPS62 double digested with BglII-KpnI, Lanes 5 and 6 are pPS55 digested with BglII and KpnI, and Lane 7 is pPS55 double digested with BglII-KpnI. In image-C, Lanes 2 and 3 are pPS43 digested with BglII and KpnI, Lane 4 is pPS43 double digested with BglII-KpnI, Lane 5 and 6 are pPS50 digested with BglII and KpnI, and Lane 7 is pPS50 double digested with BglII-KpnI.

In all three images, the single digest yields a single band of the total size of vector and insert. The vector sizes are 4.1 kb for both pAcGFP1-1 and pDsRed2-1. The amplified promoter sizes of *flhD*$_{AJW678}$, *flhD*$_{MC1000}$, and *ompR*$_{MC1000}$ are 603 bp, 1575 bp, and 456 bp, respectively. With the six double digests, gel electrophoresis produced two bands. The upper band is the vector (pAcGFP1-1 in Lane 4 and pDsRed2-1 in Lane 7, for all three gels) and the smaller fragments are the promoter fragments of the respective plasmids.

From the sizes of the restriction fragments, plasmid maps were deduced and are presented in Fig. 7.

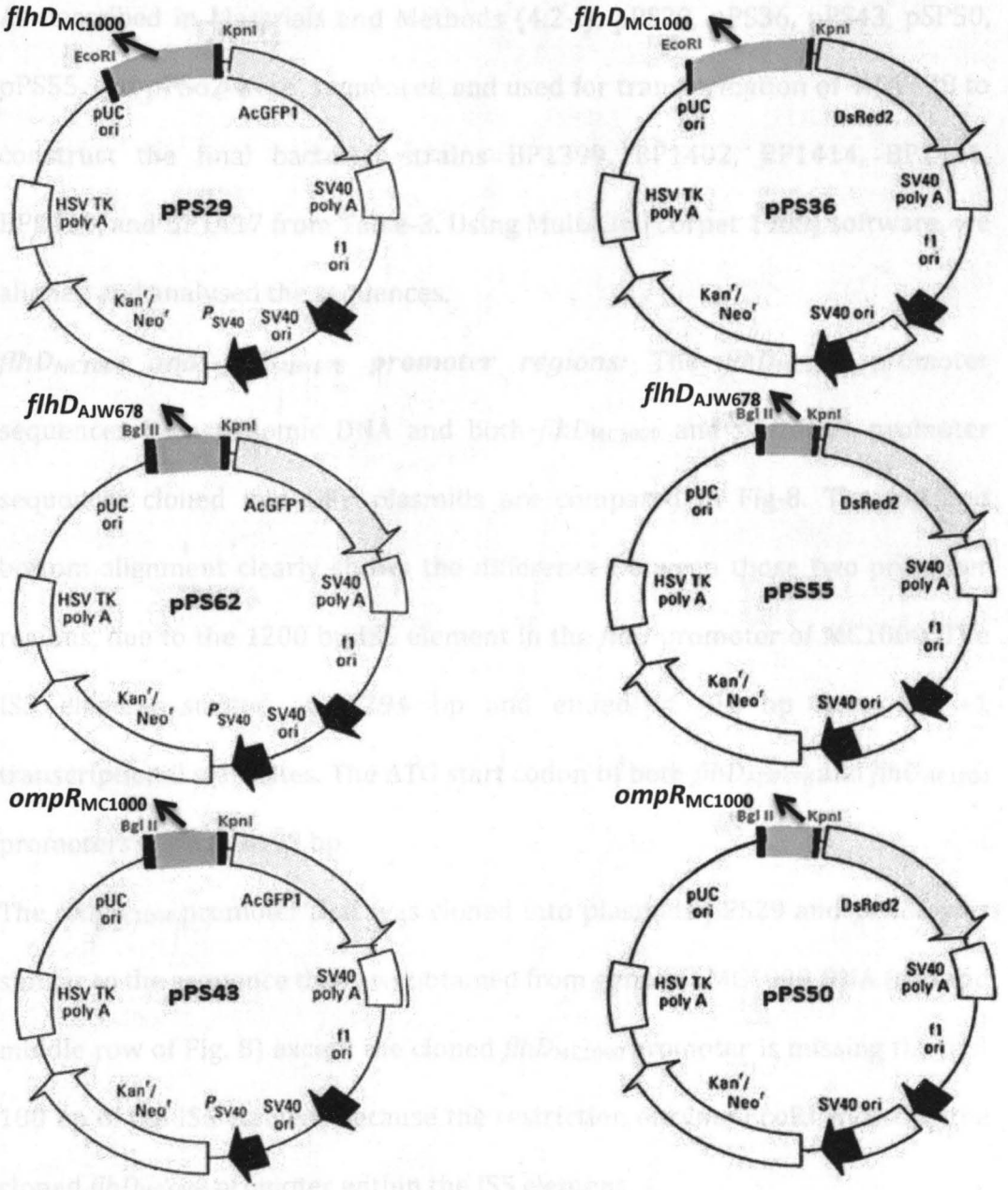

Fig - 7 ***Plasmid maps.***

On the left are the promote- fused pAcGFP1-1 plasmids and on the right are the promoter-fused pDsRed2-1 plasmids. The first row is shows the plasmids with $flhD_{MC1000}$ promoters, while the second and third rows show the plasmids with $flhD_{MC1000}$ and $ompR_{MC1000}$ promoters, respectively.

2.1.2 Sequencing result

As described in Materials and Methods (4.2-I), pPS29, pPS36, pPS43, pSP50, pPS55, and pPS62 were sequenced and used for transformation of AJW678 to construct the final bacterial strains BP1399, BP1402, BP1414, BP1411, BP1420, and BP1417 from Table-3. Using MultAlin (Corpet 1988) software, we aligned and analysed the sequences.

A. flhD$_{MC1000}$ and flhD$_{AJW678}$ promoter regions: The *flhD*$_{MC1000}$ promoter sequences from genomic DNA and both *flhD*$_{MC1000}$ and *flhD*$_{AJW678}$ promoter sequences cloned into GFP plasmids are compared in Fig-8. The top and bottom alignment clearly shows the difference between those two promoter regions, due to the 1200 bp IS5 element in the *flhD* promoter of MC1000. The IS5 element started at -1294 bp and ended at -94 bp from the +1 transcriptional start sites. The ATG start codon of both *flhD*$_{AJW678}$ and *flhD*$_{MC1000}$ promoters were at +199 bp.

The *flhD*$_{MC1000}$ promoter that was cloned into plasmids pPS29 and pPS36 was similar to the sequence that was obtained from genomic MC1000 DNA (top and middle row of Fig. 8) except the cloned *flhD*$_{MC1000}$ promoter is missing the first 100 bp of the IS5 element because the restriction enzyme EcoRI is cutting the cloned *flhD*$_{MC1000}$ promoter within the IS5 element.

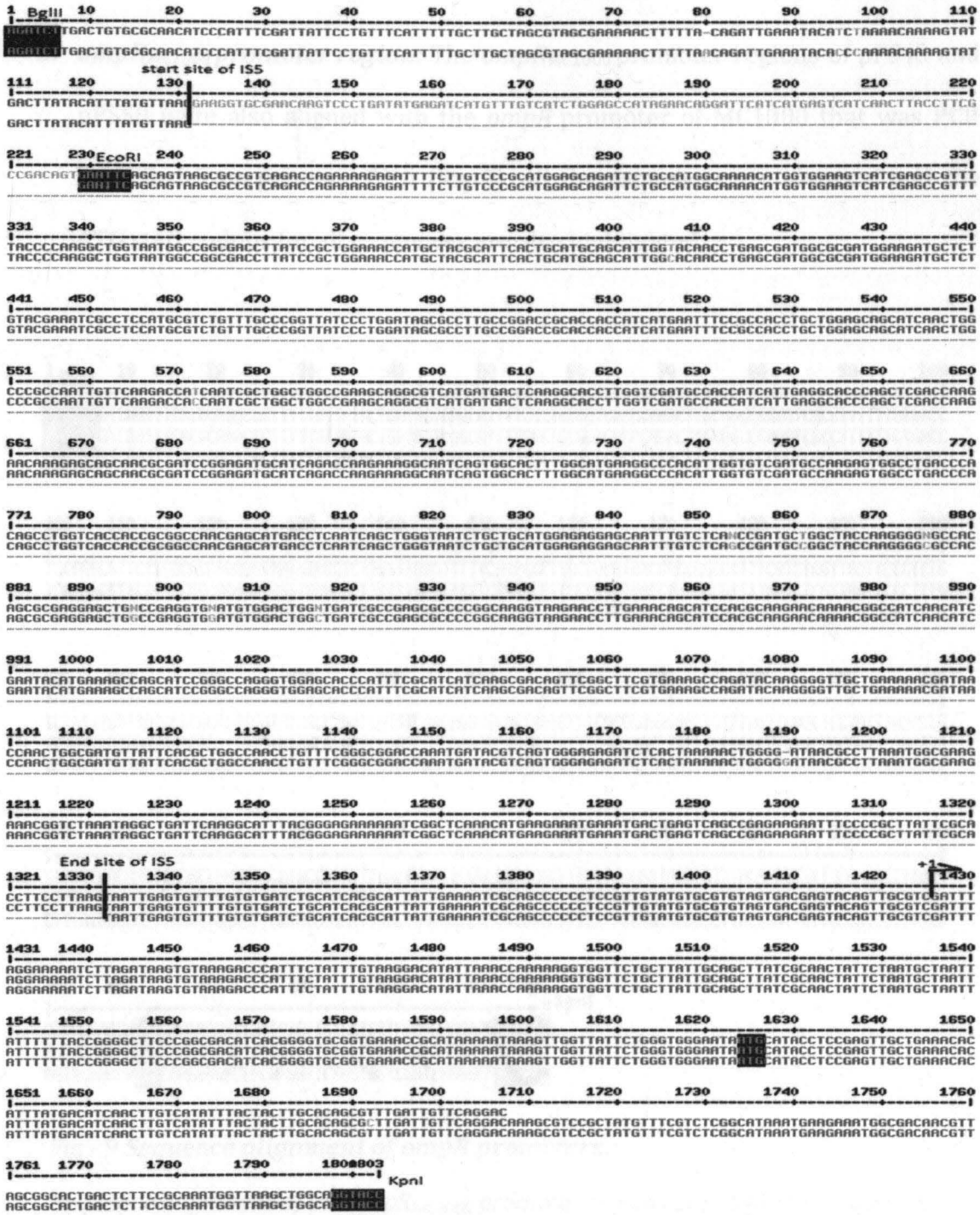

Fig - 8 ***Sequence alignment of flhD promoters.***

Sequence alignment of the $flhD_{MC1000}$ (top sequence) that was amplified from genomic DNA, and $flhD_{MC1000}$ (middle sequence) and $flhD_{AJW678}$ (bottom sequence) promoters which were cloned into GFP/RFP plasmids. Start and end of the IS5 element are indicated, as are the +1 transcriptional start site and the ATG start codon. Restriction sites are also indicated.

B. ompR$_{MC1000}$ promoter region: The *ompR*$_{MC1000}$ promoter regions of pPS43 and pPS50 were also aligned with the *ompR* promoter of MC1000 that was PCR amplified from genomic DNA (Fig-9). All the sequences are identical and the ATG start codons for all sequences are also highlighted.

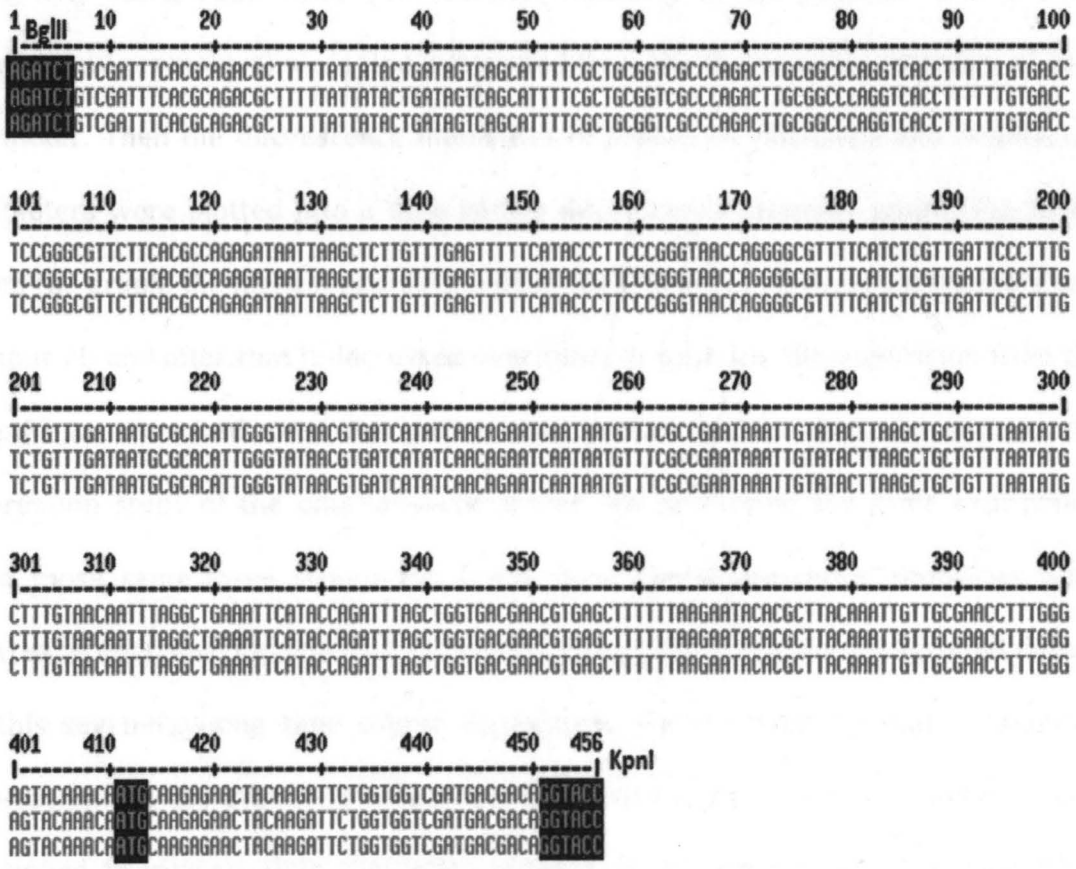

Fig - 9 ***Sequence alignment of ompR promoters.***

Sequence alignment of the ompR$_{MC1000}$ promoter regions of pPS43 (top sequence), pPS50 (middle sequence) and ompR$_{MC1000}$ (bottom sequence) promoters that were amplified from genomic DNA. The ATG start codon for all sequences is indicated.

2.2. 96-well microtiter plate assay

This experiment was performed to determine temporal expression from the respective promoters in planktonic bacteria. Using the procedures described in Materials and Methods (4.3), the time courses of expression for *flhD* and *ompR* (using strains BP1399, BP1417 and BP1414) were determined over a time period of two days. The background noise (fluorescence intensity of the plasmids that did not contain any promoters) were first subtracted from the fluorescence intensity of each promoter. Then the fluorescence intensities of $flhD_{MC1000}$, $flhD_{AJW678}$ and $ompR_{MC1000}$ promoters were plotted into a time versus fluorescence intensity graph (Fig-10-A). From the graph, the highest expression from the $flhD_{MC1000}$, $flhD_{AJW678}$ promoters was at hour 20 and after that it decreased over time. In contrast, the expression from the $ompR_{MC1000}$ increased over the entire time period of two days. To expand the expression study of the $ompR_{MC1000}$ promoter, we performed the same experiment with those same three strains for seven days. The fluorescence intensities were plotted as described for Fig-10-A (Fig-10-B), after subtracting the background noises. In this seven-day-long time course experiment, we observed the same maximum expression for the two *flhD* promoters. The expression from the *ompR* promoter continued to increase over the entire seven days. In addition, we also studied the expression from the *ompC, ompR, ackA*, and *dcuS* promoters for four days, using the BP1429, BP1430, BP1431 and BP1432 strains (Fig-10, C and D).

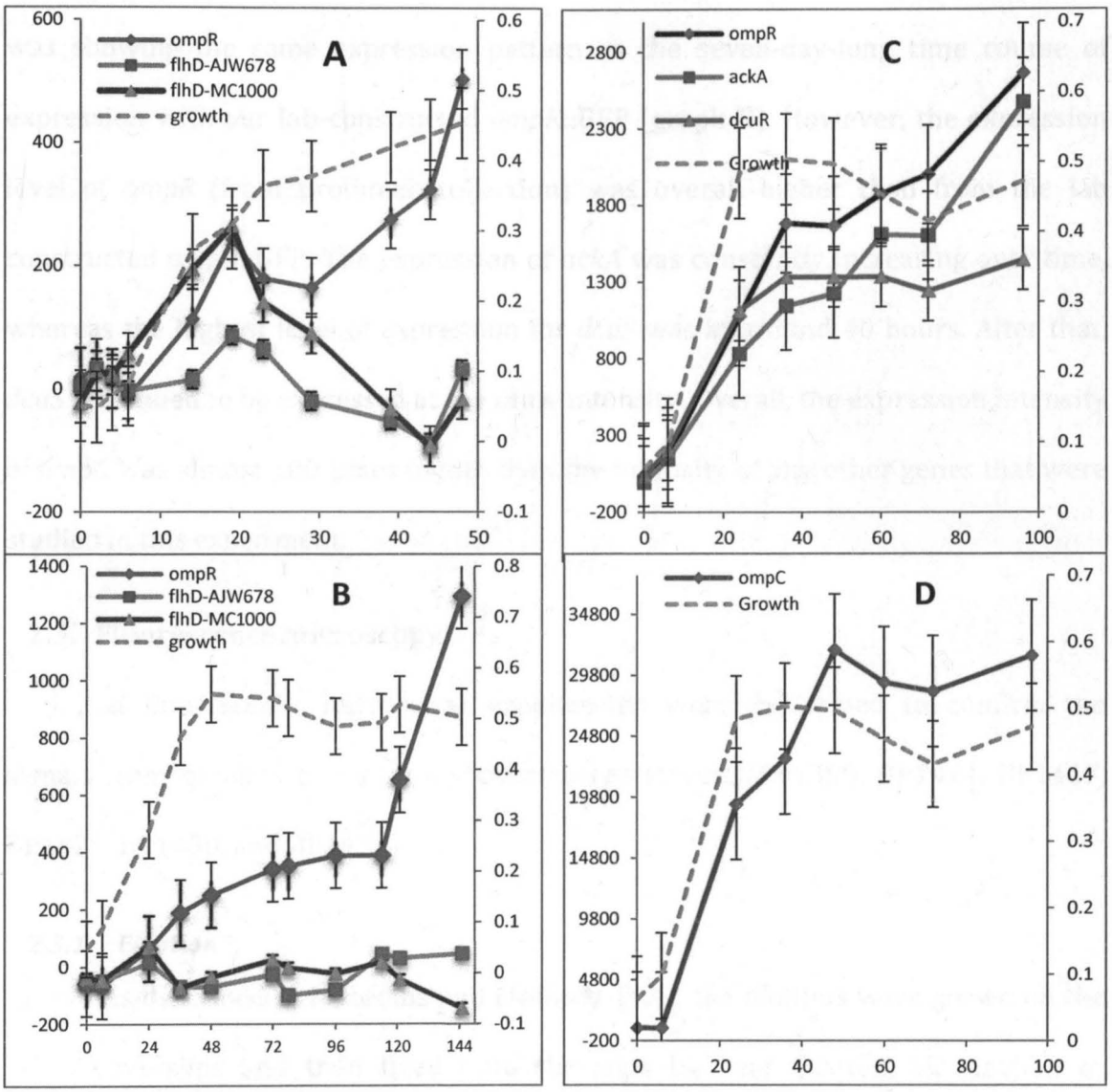

Fig - 10 ***Time course of gene expression graphs.***

Time course of gene expression for ompR and flhD (from both $flhD_{MC1000}$ and $flhD_{AJW678}$) promoters are shown in graphs-A (2 days) and B (7 days). Time course of gene expression for ompR, ackA, dcuR (graph-C) and ompC (graph-D) are also shown from day 4 of the experiment. In all four graphs, the dotted lanes are showing the average optimal density (OD) of all bacteria at 570 nm of wavelength. The ***primary Y-axis*** *is showing the fluorescence intensity,* ***secondary Y-axis*** *is showing the OD reading at 570 and the* ***X-axis*** *is showing the time in hours.*

The four-day-long time course of expression for *ompR* (from promoter collection) was showing the same expression pattern as the seven-day-long time course of expression with our lab-constructed *ompR*::GFP (graph-B). However, the expression level of *ompR* (from promoter collection) was overall higher than from the lab constructed *ompR*::GFP. The expression of *ackA* was constantly increasing over time, whereas the highest level of expression for *dcuS* was at around 40 hours. After that, *dcuS* continued to be expressed at the same intensity. Overall, the expression intensity of *ompC* was almost 100 times higher than the intensity of any other genes that were studied in this experiment.

2.3. Fluorescence microscopy

Initial fluorescence microscopy experiments were performed to confirm the signals from biofilms of the newly constructed strains (BP1399, BP1414, BP1417, BP1429, BP1430, and BP1432).

2.3.1. Fixation

As described in Materials and Methods (4.4), the biofilms were grown on the coverslips and then fixed onto the slips by heat fixation, air fixation or glutaraldehyde fixation to compare them with the unfixed control samples. Fig-11 shows images from the different fixation techniques as well as the control sample. All the biofilms were grown on to the slips using the BP1432 strain which contains the *ompC* promoter-fused GFP plasmid. Among the three different fixation techniques, glutaraldehyde fixation (D) shows the best result. In case of heat fixation (C), the signals from the biofilms were not clear. It is possible that because of the heating, the fluorescence signals of GFP plasmids

quenched out. In the case of air fixation (B), the fluorescence signals were not very sharp. Overall, in comparison to the signals from any fixation, the unfixed control samples (A) produced better signals. Among the fixations, the glutaraldehyde fixation produced the best signal.

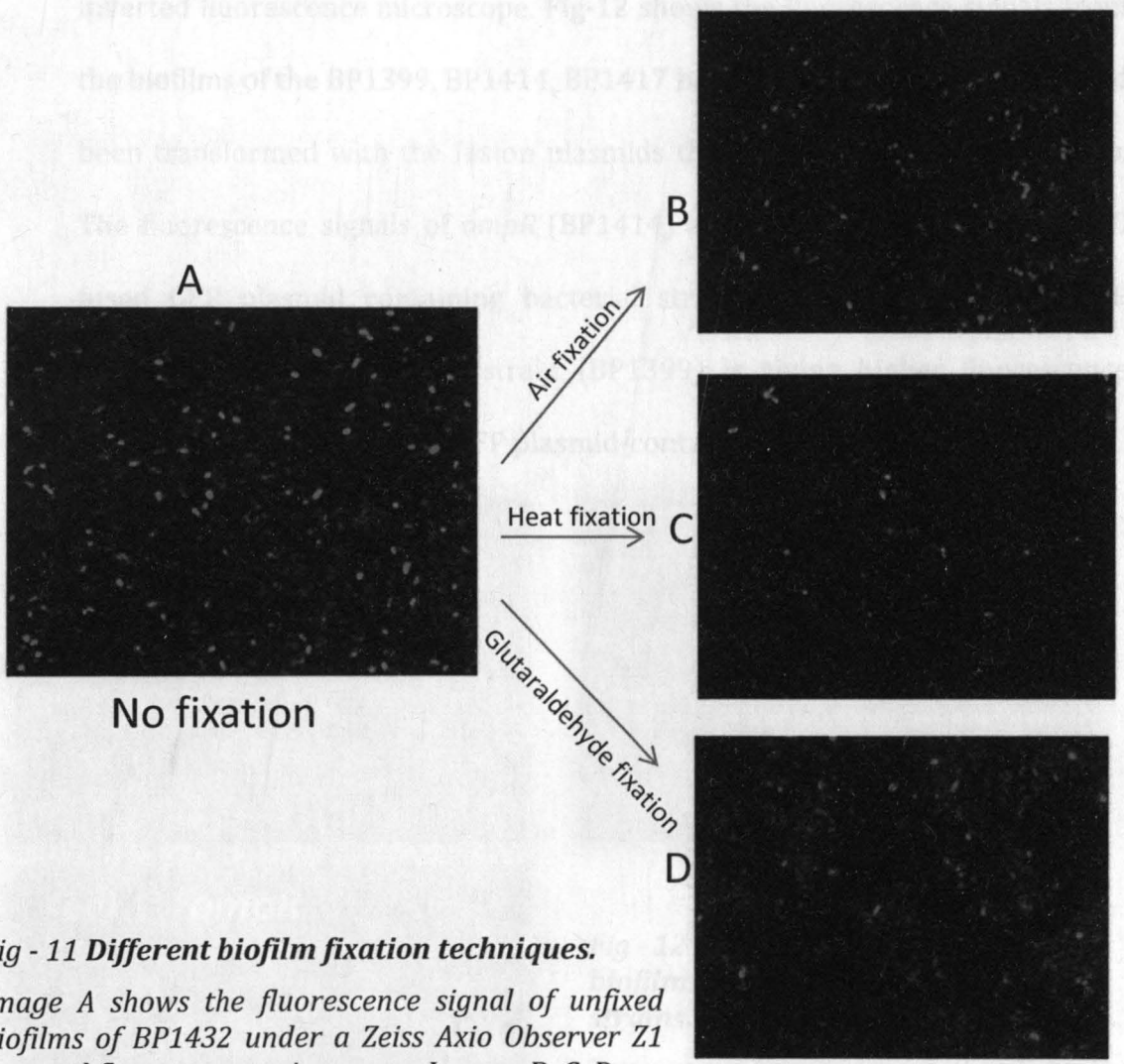

Fig - 11 ***Different biofilm fixation techniques.***

Image A shows the fluorescence signal of unfixed biofilms of BP1432 under a Zeiss Axio Observer Z1 inverted fluorescence microscope. Images B, C, D are showing the fluorescence signals of air fixed, heat fixed and glutaraldehyde fixed biofilms, respectively. All samples were excited for 400 ms at 470/40 wavelength. Emission was determined at 525/50 wavelength.

2.3.2. *Biofilm samples under fluorescence microscope*

After growing the biofilms of BP1399, BP1414, BP1417, BP1429, BP1430, and BP1432 bacterial strains on the glass slides as described in Materials and Methods (4.4.1), the samples were studied under a Zeiss Axio Observer Z1 inverted fluorescence microscope. Fig-12 shows the fluorescence signals from the biofilms of the BP1399, BP1414, BP1417 bacterial stains. These strains had been transformed with the fusion plasmids that were constructed in our lab. The fluorescence signals of *ompR* (BP1414) are much higher than both *flhD* fused GFP plasmid containing bacterial strains. The $flhD_{MC1000}$ fused GFP plasmid-containing bacterial strain (BP1399) is giving higher fluorescence signals than $flhD_{AJW678}$ fused GFP plasmid-containing bacterial strain (BP1417).

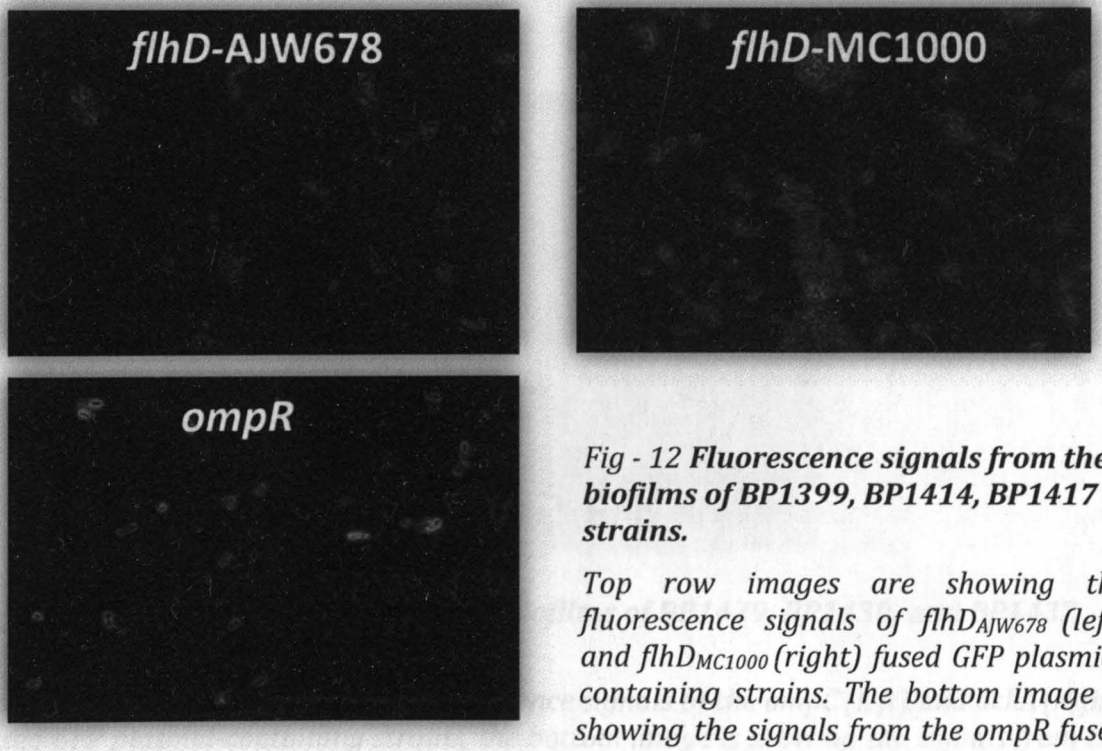

Fig - 12 ***Fluorescence signals from the biofilms of BP1399, BP1414, BP1417 strains.***

Top row images are showing the fluorescence signals of $flhD_{AJW678}$ (left) and $flhD_{MC1000}$ (right) fused GFP plasmid-containing strains. The bottom image is showing the signals from the ompR fused GFP plasmid-containing strain.

Fig-13 is showing the fluorescence signals from the biofilms of BP1429, BP1430, and BP1432 bacterial strains. These strains were transformed with the fusion plasmids from the promoter fusion collection. Both BP1429, BP1430 produced clear fluorescence signals, but the fluorescence signals of BP1432 are much higher than others.

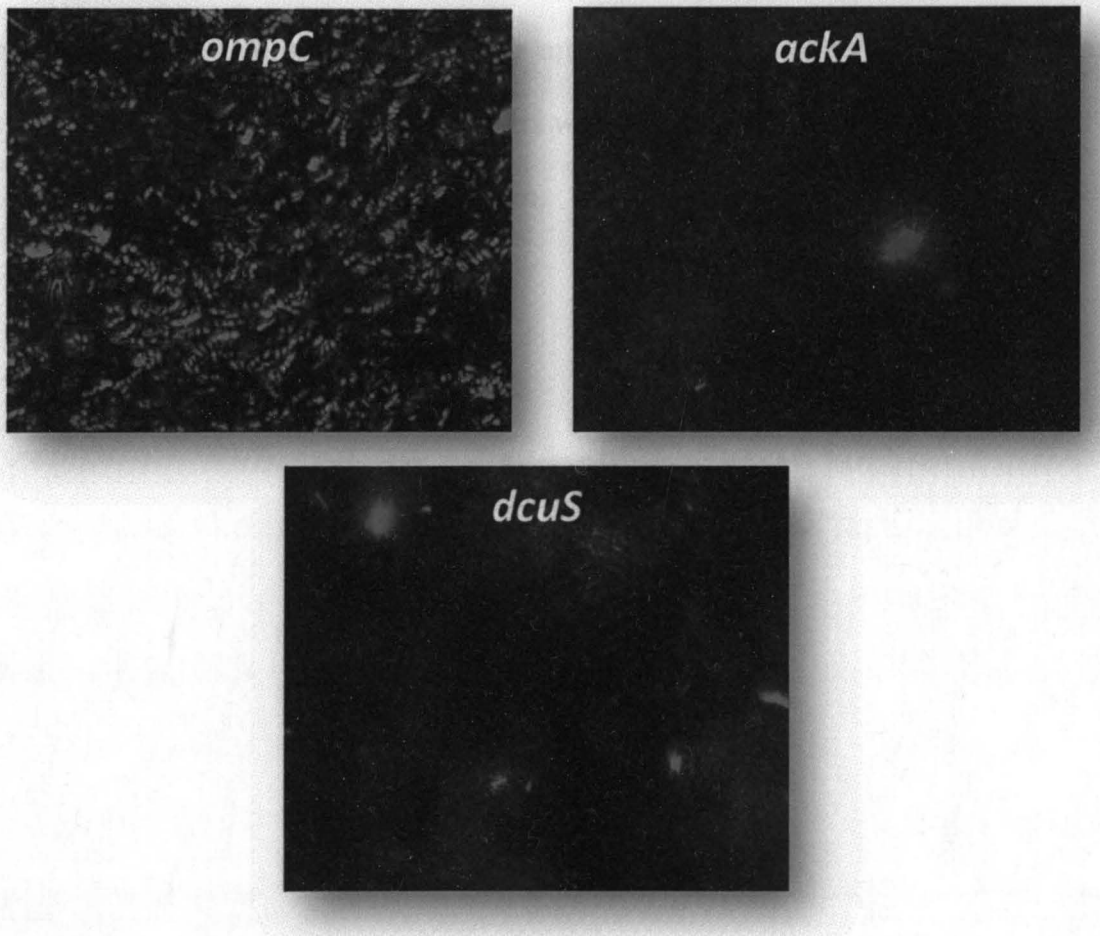

Fig - 13 ***Fluorescence signals from the biofilms of BP1429, BP1430, and BP1432 bacterial strains.***

Top row images are showing the fluorescence signals of the ompC (left) and ackA (right) fused GFP plasmid-containing strains, the bottom image is showing the signals from the dcuS fused GFP plasmid-containing strain.

All of the fluorescence signals from the biofilms of BP1429, BP1430, BP1432, BP1399, BP1414 and BP1417 bacterial strains were taken at same time point and at the same wavelength after excitation for equal time. But the Z-axis focal points for these three strains were different. For *ompC*, we took the images at the top layers of the biofilms, even though signals were seen throughout the entire biofilm. In contrast, for the *ackA* and *dcuS* promoters, the top-layer bacteria barely gave any signals. As a consequence, we took the images at the middle layer. In case of the *flhD* and *ompR* promoters, the signals from the top layers were visualized. These promoters failed to yield signals further down into the biofilm.

DISCUSSION

The goals of this study were **i.** to confirm the hypothesis from our past high-throughput quantitative biofilm experiment and the phenotype microarray experiment that acetate metabolism mutant strains may form different biofilms than their isogenic parental strain and **ii.** the construction of the required promoter fusions and bacterial strains to study the temporal expression of selected promoters. According to the first goal of the study, SEM was performed with biofilms formed by the AJW678 strain and its *ackA* and *ackA pta* mutants (acetate metabolism mutants), as well as double mutants in *ackA* and either of the response regulator genes *ompR, rcsB, or dcuR.* We confirmed that acetate metabolism has an important role in biofilm formation. In addition, this study identifies that RcsB is responsible for the structural differences between the *ackA* mutant and its parent strain, while DcuR is required for the increased biofilm amount of the *ackA* mutant. The $flhD_{AJW678}$, $flhD_{MC1000}$, $ompR_{MC1000}$ fused pAcGFP1-1 and pDsRed2-1 plasmids (pPS43, pPS50, pPS55, pPS62, pPS29, pPS36) were constructed. The *E. coli* K-12 strain AJW678 was transformed with these plasmids, as well as additional promoter::GFP fusion plasmids from the Open Biosystems collection. The activity from these promoters was first investigated with a 96-well plate assay. Initial microscopic experiments were done with those bacterial strains. Fluorescence signals were obtained from all promoters.

When *E. coli* grow on glucose based media, glucose is converted into acetyl-CoA through glycolysis. The acetyl-CoA is then converted into acetyl phosphate and acetate (Fig-14). The synthesis of acetyl phosphate is mediated by

phosphotransacetylase (Pta) and the production of acetate is catalyzed by acetate kinase (AckA) (Brown 1977). Acetyl phosphate is a high energy containing intermediate that transmits certain environmental signals to central metabolism. It can modulate the activity of some 2CSTSs by phosphorylating the response regulators (for review, see Wolfe 2005).

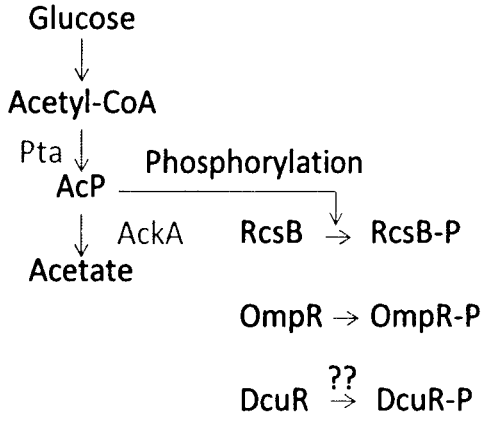

Fig - 14 ***Acetate metabolism pathway.***

Glucose is converted into acetyl-CoA by glycolysis. This is converted into acetyl phosphate (AcP) and then acetate with the help of Pta and AckA, respectively. The activated acetate intermediate AcP serves as a phosphodonor to phosphorylate response regulators, such as RcsB, OmpR, and possibly DcuR.

Both OmpR and RcsB are activated by receiving the phosphate group of the acetyl phosphate. After phosphorylation, RcsB activates the *wca* operon that is responsible for the production of colanic acid (Cano 2002), which may be a key product to control the structure of the biofilms. It will be interesting to determine whether DcuR is also activated by receiving the phosphate group of AcP and then how DcuR influences metabolism to have an impact in biofilm formation.

A previous study (Wolfe 2003) described that both *ackA* and *ackA pta* mutants can form biofilm. *ackA* mutants, which over-synthesize AcP and lack flagella form a pilus-based biofilm, whereas *ackA pta* mutants which are unable to synthesize AcP and

over-synthesize flagella form a flagella-based biofilm. The authors hypothesized that AcP may act as a metabolic signal to the bacteria which allows them to switch from reversible attachment (flagella) to irreversible attachment (fimbriae). However, the *ackA* mutant which accumulates acP and the *ackA pta* mutant which doesn't synthesize any acP, both form quantitatively and qualitatively different biofilms than their parent strain. This strongly suggests that acP is not the only acetate intermediate that is responsible for those differences. Since both acetyl-CoA (Thao 2010) and acetate (Chavez 2009) can activate 2CSTSs response regulators, it is possible that acetyl-CoA, acetate and acP together might control the activity of various 2CSTS response regulators and allow bacteria to respond to the larger variety of environmental signals.

As explained in the Literature Review, different stages of biofilm formation (Fig-2) are characterized by different extra-cellular organelles. All these organelles are regulated by different genes. Depending on the developmental stage specific organelles, the hypothesized expression of selected genes are shown in Fig- 15. During reversible attachment, bacteria are loosely attached to the surface by their flagella, and flagella are primarily controlled by *flhD/flhC*. In the case of irreversible attachment, the curli and type I fimbriae help bacteria to tightly attach to the surface, and the matured biofilm is characterized by the capsule. While FlhDC positively regulates flagella and curli, OmpR negatively regulates flagella and type I fimbriae and positively regulates curli. RcsCDB negatively regulates flagella and curli and positively regulates type 1 fimbriae and the capsule. Fig-15 shows the temporal as well as the spatial hypothesized expression of FlhDC, OmpR, and RcsCDB.

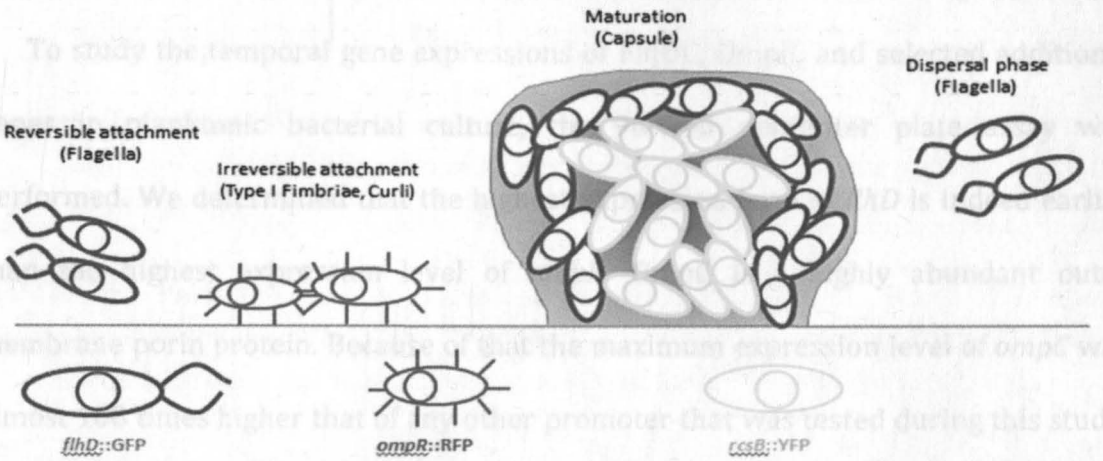

Fig - 15 ***Hypothesized gene regulation during different biofilm developmental stages.***

To study the different gene expression, the promoter region of flhD and ompR were fused in front of the ORF of GFP and RFP, respectively and the promoter region of rcsB will be fused in front of the ORF of YFP. The color of bacteria is indicating the highest expression of the promote-fused plasmids of same color.

As flagella are present at a very early stage, in terms of the temporal expression, the highest expression of FlhDC is expected earlier than OmpR and RcsCDB. Within the mature biofilm, the expression of FlhDC is expected at the outer layer, where flagellated bacteria leave the biofilm (dispersal). Expression of RcsCDB is expected in the inner layer of the matured 3D biofilms, activating the synthesis of colanic acid and keeping the biofilm together.

To test the temporal and spatial expression of FlhDC and OmpR, promoter fused GFP/RFP plasmids were cloned and AJW678 was transformed with these plasmids. The resulting strains were tested on 96-well plates and with fluorescence microscopy.

All newly constructed strains produced signals, which confirms that our constructs are working.

To study the temporal gene expressions of FlhDC, OmpR, and selected additional genes in planktonic bacterial culture, the 96-well microtiter plate assay was performed. We determined that the highest expression level of *flhD* is indeed earlier than the highest expression level of *ompR*. OmpC is a highly abundant outer membrane porin protein. Because of that the maximum expression level of *ompC* was almost 100 times higher that of any other promoter that was tested during this study. We will use this promoter as a positive control to optimize the fluorescence microscopy experiments. From the 96-well microtiter plate assay experiment, we obtained an initial estimate of the expression time of different genes, which will help us to do the fluorescence microscopy experiments later. In the future, this 96-well microtiter plate assay will be performed to quickly screen the promoters with significant changes of expression during the 7-day-long time course experiments. After the quick screen, all those promoters that produce a signal high enough to perform the fluorescence microscopy will be tested under real time fluorescence microscopy to see their effect in the biofilm formation. Overall, this study was used to make the necessary constructs that will enable us to perform future temporal and spatial gene expression studies.

BIBLIOGRAPHY

Addy, M., Slayne, M.A., Wade, W.G. *Methods for the Study of Dental Plaque Formation and Control,*. Oxford: Blackwell Scientific Publications, 1993.

Barker, C.S., Prüß, B.M., Matsumura, P. (2004) "Increased motility of *Escherichia coli* by insertion sequence element integration into the regulatory region of the *flhD* Operon." *J. Bacteriol.* 186(22): 7529–7537.

Bartlett, R.J., Pericak-Vance, M.A., Koh, J., Yamaoka, L.H., Chen, J.C., Hung, W.Y., Speer, M.C., Wapenaar, M.C., Van Ommen, G.J., Bakker, E., et al. (1988) "Duchenne muscular dystrophy: high frequency of deletions." *Neurology* 38(1): 1-4.

Borenstein, S.W. *Microbiologically Influenced Corrosion Handbook.* Cambridge: Woodhead Publishing Ltd, 1994.

Boyd, A., Chakrabarty, A.M. (1994) "Role of alginate lyase in cell detachment of *Pseudomonas aeruginosa*." *Appl. Environ. Microbiol.* 60(7): 2355-2359.

Bridier, A., Tischenko, E., Dubois-Brissonnet, F., Herry, J.M., Thomas, V., Daddi-Oubekka, S., Waharte, F., Steenkeste, K., Fontaine-Aupart, M.P., Briandet, R. (2011) "Deciphering biofilm structure and reactivity by multiscale time-resolved fluorescence analysis." *Adv. Exp. Med. Biol.* 715: 333-349.

Brombacher, E., Dorel, C., Zehnder, A.J.B., Landini, P. (2003) "The curli biosynthesis regulator CsgD co-ordinates the expression of both positive and negative determinants for biofilm formation in *Escherichia coli*." *Microbiology* 149(10): 2847-2857.

Brown, T.D., Jones-Mortimer, M.C., Kornberg, H.L. (1977) "The enzymic interconversion of acetate and acetyl-coenzyme A in *Escherichia coli*." *J. Gen. Microbiol.* 102(2): 327-36.

Cano, D.A., Domínguez-BernaL, G., Tierrez, A., Garcia-Del Portillo, F., Casadesús, J. (2002) "Regulation of capsule synthesis and cell motility in *Salmonella enterica* by the essential gene *igaA*." *Genetics* 162(4): 1513-1523.

Charlot, A.F., Cornet, M.P.C., Gutierrez, C., Cam, K. (2005) "Osmotic regulation of the *Escherichia coli* bdm (Biofilm-Dependent Modulation) gene by the RcsCDB His-Asp phosphorelay." *J. Bacteriol.* 187(11): 3873–3877.

Chavez, R.G., Alvarez, A.F., Romeo, T., Georgillis, D. (2010) "The physiological stimulus for the BarA sensor kinase." *J. Bacteriol.* 192(7):2009–2012

Combaret, C.P., Brombacher, E., Vidal, O., Ambert, D.A., Lejeune, P., Landini, P., Dorel, C. (2001) "Complex Regulatory Network Controls Initial Adhesion and Biofilm Formation in *Escherichia coli* via Regulation of the *csgD* Gene." *J. Bacteriol.* 183(24): 7213-7223.

Corpet, F. (1988) "Multiple sequence alignment with hierarchical clustering." *Nucl. Acids Res.* 16(22): 10881-10890.

Danese, P.N., Pratt, L.A., Kolter,R. (2000) "Exopolysaccharide production is required for development of *Escherichia coli* K-12 biofilm architecture." *J. Bacteriol.* 182(12): 3593–3596.

Drake, L.A., Doblin, M.A., Dobbs, F.C. (2007) "Potential microbial bioinvasions via ships' ballast water, sediment, and biofilm." *Mar. Pollut. Bull.* 55(7-9): 333-341.

Ferrières, L., Clarke, D.J. (2003) "The RcsC sensor kinase is required for normal biofilm formation in *Escherichia coli* K-12 and controls the expression of a regulon in response to growth on a solid surface." *Mol. Microbiol.* 50(5): 1665–1682.

Francez-Charlot, A., Laugel, B., Van Gemert, A., Dubarry, N., Wiorowski, F., Castanié-Cornet, M.P., Gutierrez, C., Cam, K. (2003) "RcsCDB His-Asp phosphorelay system negatively regulates the flhDC operon in *Escherichia coli*." *Mol. Microbiol.* 49(3): 823-832.

Gao, R., Mack, T.R., Stock, A.M. (2007) "Bacterial response regulators:versatile regulatory strategies from common domains." *Trends. Biochem. Sci.* 32(5): 225-234.

Gil, G.C., Chang, I.S., Kim, B.H., Kim, M., Jang, J.K., Park, H.S., Kim, H.J. (2003) "Operational parameters affecting the performannce of a mediator-less microbial fuel cell." *Biosens. Bioelectron.* 18(4): 327-334.

Golby, P., Davies, S., Kelly, D.J., Guest, J.R., Andrews, S.C. (1999) "Identification and characterization of a two-component sensor-kinase and response-regulator system (DcuS-DcuR) controlling gene expression in response to C4-dicarboxylates in *Escherichia coli*." *J. Bacteriol.* 181(4): 1238-1248.

Gottesman, S., Trisler, P., Torres-Cabassa, A. (1985) "Regulation of capsular polysaccharide synthesis in *Escherichia coli* K-12: characterization of three regulatory genes." *J. Bacteriol.* 162(3): 1111-1119.

Janausch, I.G., Zientz, E., Tran, Q.H., Kröger, A., Unden, G. (2002) "C4-dicarboxylate carriers and sensors in bacteria." *Biochim. Biophys. Acta.* 1553(1-2): 39-56.

Krämer, J., Fischer, J.D., Zientz, E., Vijayan, V., Griesinger, C., Lupas, A., Unden, G. (2007) "Citrate sensing by the C4-dicarboxylate/citrate sensor kinase DcuS of *Escherichia coli*: binding site and conversion of DcuS to a C4-dicarboxylate- or citrate-specific sensor." *J. Bacteriol.* 189(11): 4290–4298.

Kumari, S., Beatty, C.M., Browning, D.F., Busby, S.J., Simel, E.J., Hovel-Miner, G., Wolfe, A.J. (2000) "Regulation of acetyl coenzyme A synthetase in *Escherichia coli*." *J. Bacteriol.* 182(15): 4173-4179.

Legnani, D. (2009) "Acute bacterial exacerbation of chronic obstructive pulmonary disease and biofilm." *Infez. Med.* 17(6): 10-19.

Li, J., Helmerhorst, E., Leone, C., Troxler, R., Yaskell, T., Haffajee, A., Socransky, S., Oppenheim, F. (2004) "Identification of early microbial colonizers in human dental biofilm." *J. Appl. Microbiol.* 97(6): 1311–1318.

Maeda, S., Mizuno, T. (1990) "Evidence for multiple OmpR-binding sites in the upstream activation sequence of the ompC promoter in *Escherichia coli*: a single OmpR-binding site is capable of activating the promoter." *J. Bacteriol.* 172(1): 501-503.

Marquisa, S.M., Stantona, B.A., O'Toole, G.A. (2008) "*Pseudomonas aeruginosa* biofilm formation in the cystic fibrosis airway." *Pulm. Pharmacol. Ther.* 21(4): 595-599.

Mascher, T., Helmann, J.D., Unden, G. (2006) "Stimulus perception in bacterial signal-transducing histidine kinases." *Microbiol. Mol. Biol. Rev.* 70(4): 910–938.

Mikkelsen, H., Sivaneson, M., Filloux, A. (2011) "Key two-component regulatory systems that control biofilm formation in *Pseudomonas aeruginosa*." *Environ. Microbiol.* 13(7): 1666-1681.

Moat, A.G.,Foster, J.W., Spector M.P. *Microbial physiology.* New York: Wiley-Liss, 2002.

Monroe, D. (2007) "Looking for chinks in the armor of bacterial biofilms." *PLoS Biol.* 5(11): 2458-2461.

Murphy, T.F. (2008) "Chronic *Pseudomonas aeruginosa* infection in chronic obstructive pulmonary disease." *Clin. Infect. Dis.* 47(12): 1526-1533.

Nett, J., Lincoln, L., Marchillo, K., Andes, D. (2007) "Beta -1,3 glucan as a test for central venous catheter biofilm infection." *J. Infect. Dis.* 195(11): 1705-1712.

Njoroge, J., Sperandio, V. (2009) "Jamming bacterial communication: New approaches for the treatment of infectious diseases." *EMBO Mol. Med.* 1(4): 201-210.

Office of Naval, research. "New hull coatings for Navy ships cut fuel use, protect environment." *eurekalert.org.* june 4, 2009. http://www.eurekalert.org/pub_releases/2009-06/oonr-nhc060409.php.

O'Toole, G., Kaplan, H.B., Kolter, R. (2000) "Biofilm formation as microbial development." *Annu. Rev. Microbiol.* 54: 49-79.

Pan, J., Ren, D. (2009) "Quorum sensing inhibitors: a patent overview." *Expert. Opin. Ther. Pat.* 19(11): 581-601.

Parkinson, J.S. (1993) "Signal transduction schemes of bacteria." *Cell* 73(5): 857-871.

Potera, C. (1998) "Studying slime." *Environ. Health Perspect.* 106(12): 604-606.

Poulsen, L.K., Ballard, G., Stahl, D.A.,. (1993) "Use of rRNA fluorescence in situ hybridization for measuring the activity of single cells in young and established biofilms." *Appl. Environ. Microbiol.* 59(5): 1354-1360.

Prüβ, B.M. (2000) "FlhD, a transcriptional regulator in bacteria." *Rece. Resear. Develop. Microbiol.* 4: 31-42.

Prüβ, B.M., Campbell, J.W., Van Dyk, T.K., Zhu, C., Kogan, Y., Matsumura, P. (2003) "FlhD/FlhC is a regulator of anaerobic respiration and the Entner-Doudoroff pathway through induction of the methyl-accepting chemotaxis protein Aer." *J. Bacteriol.* 185(2): 534-543.

Prüβ, B.M., Verma, K., Samanta, P., Sule, P., Kumar, S., Wu, J., Horne, S.M., Christianson, D., Stafslien, S.J., Wolfe, A.J., Denton, A.M. (2010) "Environmental and genetic factors that contribute to *Escherichia coli* K-12 biofilm formation." *Arch. Microbiol.* 192(9): 715-728.

Raad, I., Costerton, W., Sabharwal, U., Sacilowski, M., Anaissie, W., Bodey, G. (1993) "Ultrastructural analysis of indwelling vascular catheters: a quantitative relationship between luminal colonization and duration of placement." *J. Infect. Dis.* 168(2): 400-407.

Raad, II., Sabbagh, M.F., Rand, K.H., Sherertz, R.J. (1992) "Quantitative tip culture methods and the diagnosis of central venous catheter-related infections." *Diagn. Microbiol. Infect. Dis.* 15(1): 13-20.

Reguera, G., Nevin, K., Nicoll, J.S., Covalla, S.F. (2006) "Biofilm and nanowire production leads to increased current in *Geobacter* sulfurreducens fuel cells." *Appl. Environ. Microbiol.* 72(11): 7345-7348.

Sand, W., Gerke, T., Hallmann, R., Schippers, A. (1995) "Sulfur chemistry, biofilm, and the (in)direct attack mechanism — a critical evaluation of bacterial leaching." *Appl. Microbiol. Biotech.* 43(6): 961-966.

Shin, S., Park, C. (1995) "Modulation of flagellar expression in *Escherichia coli* by acetyl phosphate and the osmoregulator OmpR." *J. Bacteriol.* 177(16): 4696-4702.

Singh, P.K., Schaefer, A.L., Parsek, M.R., Moninger, T.O., Welsh, M.J., Greenberg, E.P. (2000) "Quorum-sensing signals indicate that cystic fibrosis lungs are infected with bacterial biofilms." *Nature* 407(6805): 762-764.

Srinivasan, A., Uppuluri, P., Lopez-Ribot, J., Ramasubramanian, A.K. (2011) "Development of a high-throughput candida albicans biofilm Chip." *PLoS One* 6(4): e19036.

Stout, V., Gottesman, S. (1990) "RcsB and RcsC: a two-component regulator of capsule synthesis in *Escherichia coli*." *J. Bacteriol.* 172(2): 659-669.

Sule, P., Horne, S.M., Logue, C.M., Prüß, B.M. (2011) "Regulation of cell division, Biofilm formation, and virulence by FlhC in *Escherichia coli* 0157:H7 Grown on meat." *Appl. Environ. Microbiol.* 77(11): 3653-3662.

Sule, P., Wadhawan, T., Carr, N.J., Horne, S.M., Wolfe, A.J., Prüss, B.M. (2009) "A combination of assays reveals biomass differences in biofilms formed by *Escherichia coli* mutants." *Lett. Appl. Microbiol.* 49(3): 299-304.

Thao, S., Chen, C.S., Zhu, H., Escalante-Semerena, J.C. (2010) "Nε-lysine acetylation of a bacterial transcription factor inhibits its DNA-binding activity." *PLoS One.* 5(12): e15123.

Wang, A., Athan, E., Pappas, P.A., Fowler, V.G., Olaison, L., Paré, C., Almirante, B., Muñoz, P., Rizzi, M., Naber, C., Logar, M., Tattevin, P., Iarussi, D.L., Selton-Suty, C., Jones, S.B., Casabé, J., Morris, A., Corey, G.R., Cabell, C.H. (2007) "Contemporary clinical profile and outcome of prosthetic valve endocarditis." *JAMA.* 297(12): 1354-1361.

Wolanin, P.M., Thomason, P.A., Stock, J.B. (2002) "Histidine protein kinases: key signal transducers outside the animal kingdom." *Genome Biol.* 3(10): 3013.1–3013.8.

Wolfe, A.J., Chang, D.E., Walker, J.D., Seitz-Partridge, J.E., Vidaurri, M.D., Lange, C.F., Prüss, B.M., Henk, M.C., Larkin, J.C., Conway, T. (2003) "Evidence that acetyl phosphate functions as a global signal." *Mol. Microbiol.* 48(4): 977-988.

Wolfe, A.J. (2005) "The acetate switch." *Microbiol. Mol. Biol. Rev.* 69(1): 12-50.

Wu, J.A., Kusuma, C., Mond, J.J., Kokai-Kun, J.F. (2003) "Lysostaphin disrupts Staphylococcus aureus and Staphylococcus epidermidis biofilms on artificial surfaces." *Antimicrob. Agents Chemother.* 47(11): 3407-3414.

Zaslaver, A., Bren, A., Ronen, M., Itzkovitz, S., Kikoin, I., Shavit, S., Liebermeister, W., Surette, M.G., Alon, U. (2006) "A comprehensive library of fluorescent transcriptional reporters for *Escherichia coli*." *Nat. Methods.* 3(8): 623-628.

Zientz, E., Bongaerts, J., Unden, G. (1998) "Fumarate regulation of gene expression in Escherichia coli by the DcuSR (dcuSR genes) two-component regulatory system." *J. bacteriol.* 180(20): 5421-5445.